AD NUMBER
AD395666
CLASSIFICATION CHANGES
TO: **UNCLASSIFIED**
FROM: **CONFIDENTIAL**
LIMITATION CHANGES
TO: **Approved for public release; distribution is unlimited.**
FROM: **Distribution authorized to U.S. Gov't. agencies and their contractors; Administrative/Operational Use; FEB 1969. Other requests shall be referred to Arnold Engineering Development Center, Arnold AFB, TN.**
AUTHORITY
AEDC ltr 7 Mar 1975 ; AEDC ltr 7 Mar 1975

DECLASSIFIED / UNCLASSIFIED

AEDC-TR-69-9

[redacted]

C#1

ARCHIVE COPY
DO NOT LOAN

WIND TUNNEL TESTS OF A TWO-THIRDS SCALE NASA HRE INLET AT MACH NUMBERS 4, 5, 6, AND 8 (U)

Frederick K. Hube and Paul J Bontrager

ARO, Inc.

[redacted] Year Intervals. [redacted] On December 31, 1975

February 1969

This document has been approved for public release its distribution is unlimited.

Per AF letter dtd March, 75 signed William O. Cole

In addition to security requirements which must be met, this document is subject to special [redacted] controls and each transmittal to [redacted] governments or foreign nationals may be [redacted] with prior approval of NASA Langley [redacted], Langley AFB, Virginia 23365.

This material contains information [redacted] national defense of the United States [redacted] the meaning of the Espionage Laws (Title [redacted] U.S.C., sections 793 and 794) the transmission [redacted] revelation of which in any manner to an [redacted] person is prohibited by law.

NATIONAL [redacted] ATION
Unau[redacted] Subject
to Criminal Sanctions

BY AUTHORITY OF
BY Linda Smith, Clerk
Name and Position of Individual
Date 2/27/75

VON KÁRMÁN GAS DYNAMICS FACILITY
ARNOLD ENGINEERING DEVELOPMENT CENTER
AIR FORCE SYSTEMS COMMAND
ARNOLD AIR FORCE STATION, TENNESSEE

DECLASSIFIED / UNCLASSIFIED

GROUP 4
Downgraded at 3 [redacted] intervals;
Declass[redacted] after 12 years.
[redacted] DIR 5200.10

[redacted]

NOTICES

When U. S. Government drawings specifications, or other data are used for any purpose other than a definitely related Government procurement operation, the Government thereby incurs no responsibility nor any obligation whatsoever, and the fact that the Government may have formulated, furnished, or in any way supplied the said drawings, specifications, or other data, is not to be regarded by implication or otherwise, or in any manner licensing the holder or any other person or corporation, or conveying any rights or permission to manufacture, use, or sell any patented invention that may in any way be related thereto.

Qualified users may obtain copies of this report from the Defense Documentation Center.

References to named commercial products in this report are not to be considered in any sense as an endorsement of the product by the United States Air Force or the Government.

Do not return this copy. When not needed, destroy in accordance with pertinent security regulations.

WIND TUNNEL TESTS OF A TWO-THIRDS SCALE NASA HRE INLET AT MACH NUMBERS 4, 5, 6, AND 8 (U)

Frederick K. Hube and Paul J Bontrager

ARO, Inc.

FOREWORD

(U) The work reported herein was done at the request of the National Aeronautics and Space Administration (NASA), Langley Research Center, Langley Air Force Base, Virginia, for the Lockheed California Company under Program Area 921E.

(U) The results of tests presented were obtained by ARO, Inc. (a subsidiary of Sverdrup & Parcel and Associates, Inc.), contract operator of the Arnold Engineering Development Center (AEDC), Air Force Systems Command, Arnold Air Force Station, Tennessee, under Contract F40600-69-C-0001. The tests were conducted during a period from March 28 to September 18, 1968, under ARO Project No. VT1861, and the manuscript was submitted for publication on December 4, 1968.

(U) This report contains no classified information extracted from other classified documents.

(U) This technical report has been reviewed and is approved.

Eugene C. Fletcher
Lt Col, USAF
AF Representative, VKF
Directorate of Test

Roy R. Croy, Jr.
Colonel, USAF
Director of Test

UNCLASSIFIED ABSTRACT

(U) An axisymmetric, variable geometry, two-thirds scale model of a NASA Hypersonic Research Engine (HRE) inlet was tested at Mach numbers 4, 5, 6, and 8. Surface pressures and temperatures were measured on the inlet centerbody and inside the cowl. Pitot pressure measurements were made at four stations along the internal passage. The measurements were obtained for various cowl positions at free-stream Reynolds numbers from 1.08×10^6 to 5.76×10^6 (based on a 12-in. cowl diameter) and over an angle-of-attack range from -5 to +5 deg. The model walls were internally cooled and maintained at a minimum frost-free condition at each test condition. Selected results are presented to illustrate the effects of cowl position, angle of attack, Mach number, and Reynolds number on the surface and rake station measurements. Inlet performance data at design operating conditions are also presented.

CONTENTS

ILLUSTRATIONS

APPENDIX
TABLES

NOMENCLATURE

A	Area, in.^{2}
C_D	Spillage drag coefficient, drag/$q_\infty A_C$
CR	Contraction ratio, ratio of cowl (capture) area to minimum throat area
D	Inlet cowl diameter, 12.00 in.
h	Duct height at rake stations, in.

K	Axial distance from mass flow shell position to fully closed position (see Fig. 2a), in.
M	Mach number
$\dot{m}$	Mass flow, lb_m/sec
p	Pressure, psia
R	Radius, in.
Re_d	Reynolds number based on probe diameter
$Re_{\infty,D}$	Free-stream Reynolds number based on cowl diameter
r	Temperature recovery factor
T	Temperature, ^oR
u	Velocity, ft/sec
x	Distance along centerline of centerbody from the apex of 10-deg cone section, in.
y	Vertical height from surface, in.
α	Angle of attack, deg
η_A	Area weighted total pressure recovery ratio
$\eta_{\dot{m}}$	Mass weighted total pressure recovery ratio
θ	Internal cowl lip angle, deg
ϕ	Rake angular location looking downstream (see Fig. 2a), deg
ρ	Density, lb_m/ft^3

SUBSCRIPTS

1,2,3	Rake stations
CB	Centerbody
c	Capture station
e	Exit station
L	Lip

o	Tunnel stilling chamber conditions
p	Pitot pressure
R	Conditions at rake station
s	Local static conditions
t	Local total conditions
w	Wall conditions
∞	Tunnel free-stream conditions

SECTION I
INTRODUCTION

(U) Chemical propulsion studies conducted in recent years have shown the potential of supersonic combustion ramjet engines for high Mach number operation. Earlier ramjet studies had already established that the capabilities of engines which burned fuel in a subsonic stream decreased rapidly at flight Mach numbers above approximately six. It followed that a hypothetical engine which could operate most efficiently over a wide Mach number range would have both subsonic and supersonic burning capabilities, that is, a dual-mode engine.

(U) A number of organizations within the aerospace industry have studied the three main engine components (inlet, combustor, and nozzle) to optimize a dual-mode engine configuration. The National Aeronautics and Space Administration (NASA) organized the Hypersonic Research Engine Program (HRE) to consolidate component results with the ultimate aim of producing an operational flight-weight research engine.

(U) The objective of the HRE program is to produce an engine which will start and operate over a Mach number range from 4 to 8. Over such a wide flight speed range, an inlet configuration which has adequate contraction ratios for high Mach number compression may not capture sufficient air at low Mach numbers. Consequently, the HRE inlet was designed with a translatable centerbody to control the mass flow characteristics. A combination of the translating centerbody and a drooping cowl lip will allow the inlet to be closed off. Eliminating airflow through the engine during power-off flight will reduce cooling requirements and save fuel since the engine is regeneratively cooled.

(U) The tests reported herein were devoted to determining the performance of a two-thirds scale HRE inlet and were a continuation of earlier one-third scale tests reported in Ref. 1. Wall temperatures and static pressures along the centerbody and inner cowl surfaces were measured. The model cowl and centerbody surfaces were internally cooled with gaseous nitrogen, and wall temperatures were maintained at a minimum frost-free level (which resulted in T_w/T_o ratios ranging from 0.15 to 0.70 on the forward centerbody and 0.75 to 0.85 near the cowl lip). Pitot pressure distributions were measured at two stations in the internal passage at Mach numbers 4 and 5 and at four stations at Mach numbers 6 and 8.

(U) The tests were conducted in the Gas Dynamic Wind Tunnels, Supersonic (A) and Hypersonic (B) of the von Kármán Gas Dynamics

Facility (VKF), AEDC. Performance tests were performed at nominal Mach numbers of 4, 5, 6, and 8 and spillage drag data were obtained at Mach number 3. Test Reynolds numbers, chosen to match full-scale flight Reynolds numbers, ranged from 1.08 x 10^6 to 5.76 x 10^6 (based on a cowl lip diameter of 12 in.), and the model angle of attack was varied from -5 to +5 deg. At Mach number 8, helium (simulated fuel) was injected into the duct to determine the blockage effects of fuel jets.

SECTION II
APPARATUS

2.1 MODEL

(U) The two-thirds scale HRE model (nominal lip diameter of 12 in.) was supplied by the Lockheed California Company. The model, shown in Fig. 1a, was constructed primarily of 17-4PH stainless steel. Throat and exit areas were varied by translating the cowl and mass flow shell, respectively. Figure 1b illustrates the actuator motor mechanisms used to translate the cowl and mass flow shell. The model exit area and the coolant exhaust are shown in Fig. 1c.

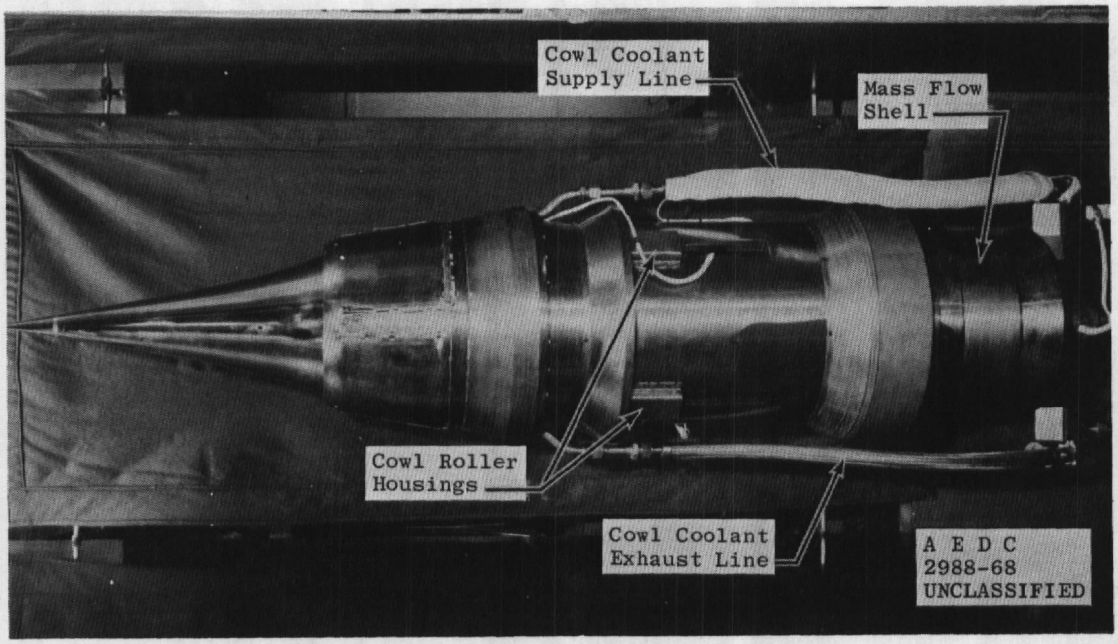

a. Model Installed in Tunnel A

Fig. 1 Model Photographs

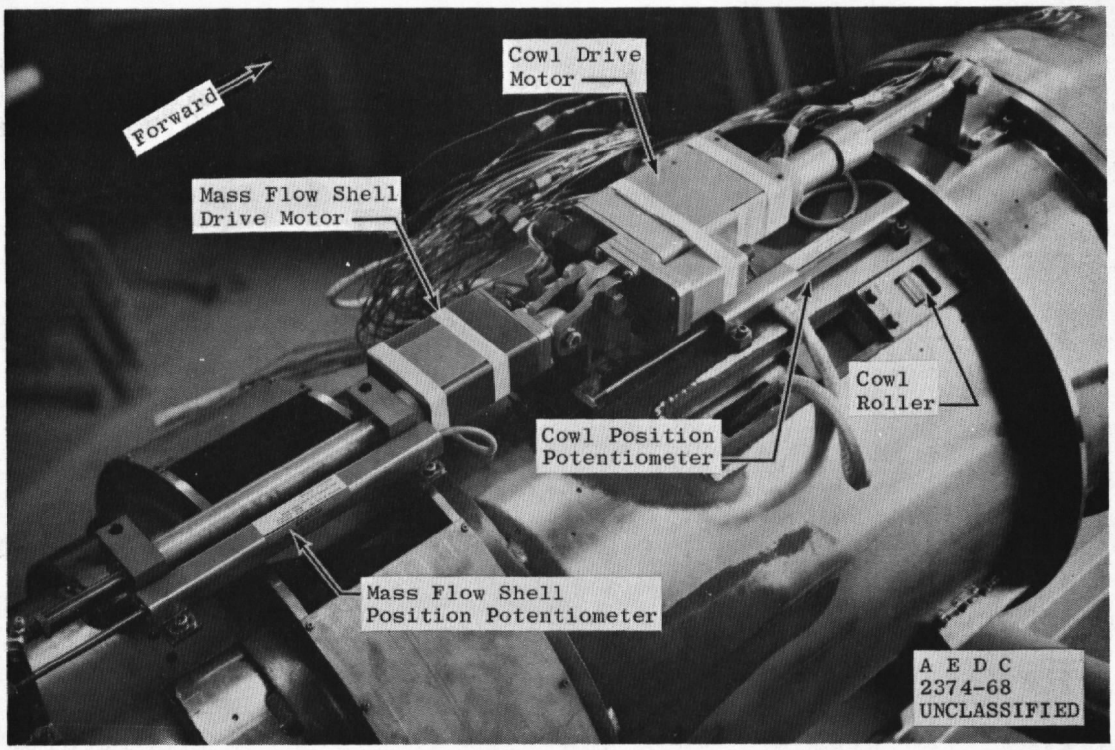

b. Cowl and Mass Flow Shell Actuator System

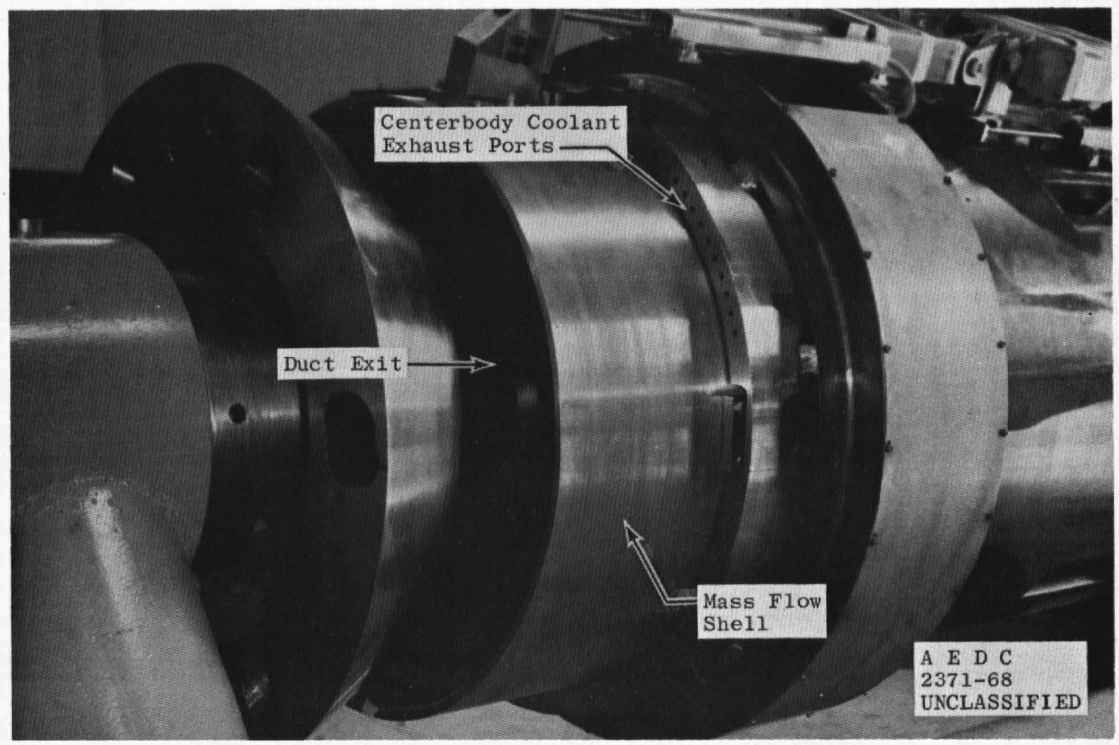

c. Exit Area Detail

Fig. 1 Concluded

(U) The drawing in Fig. 2a illustrates the contours of the inlet, and Figs. 2b through e show the variety of interchangeable components used in the preliminary tests. Inlet scaling includes centerbody, cowl lip, and internal contours back to station 27.00. The individual component selected for the final configuration is indicated in each figure. The doubler bands, Fig. 2e, represented fairing strips designed to cover joints in the full-scale inlet.

(U) Rakes (ϕ = 0, 90 deg) used to obtain pitot pressure and total temperature distributions across the duct are illustrated in Fig. 3. During the tests at Mach numbers 4 and 5, only the station 3 and 4 rakes were installed. At Mach numbers 6 and 8, rakes were installed at all stations (1 through 4). The spillage drag rake (Fig. 3c) was utilized only during the Mach number 3 tests. Additional instrumentation consisted of 52 static pressure taps and 46 surface thermocouples (see Fig. 2a).

(U) Centerbody and cowl surfaces were cooled by circulating cold gaseous nitrogen through passages under the skin as shown in Fig. 4. Liquid nitrogen was transferred from a storage tank by a variable speed pump to a steam heated vaporizer. The system outlet temperature was controlled by varying the ratio between the quantity of nitrogen sent through the vaporizer and the quantity routed around the vaporizer through a bypass. Additional control was achieved with throttling valves in the cowl and centerbody supply lines.

(U) Simulated fuel injection tests were performed at Mach number 8 to determine fuel jet blockage effects on the inlet flow. Figure 5 shows a drawing and photograph of the injection port pattern. The 0.067-in.-diam ports were arranged in two rows of 360 ports each. Helium was used to simulate the hydrogen fuel used in the full-scale engine, and flow rates were measured with a sonic orifice.

2.2 WIND TUNNELS

(U) The 40-in. supersonic and 50-in. hypersonic tunnels are continuous, closed-circuit, variable density wind tunnels. Tunnel A has an automatically driven, flexible-plate-type nozzle and a 40- by 40-in. test section. The tunnel can be operated at Mach numbers from 1.5 to 6 at maximum stagnation pressures from 29 to 200 psia, respectively, and stagnation temperatures up to 750°R (M_∞ = 6). Minimum operating pressures range from about one-fourth to one-twentieth of the maximum at each Mach number.

	Static Pressures	Surface Thermocouples	Station Location
Centerbody	21	27	12 → 39.66
Cowl	23	11	Cowl Leading Edge to 15 in. Aft of Leading Edge
Diffuser	8	8	64.50

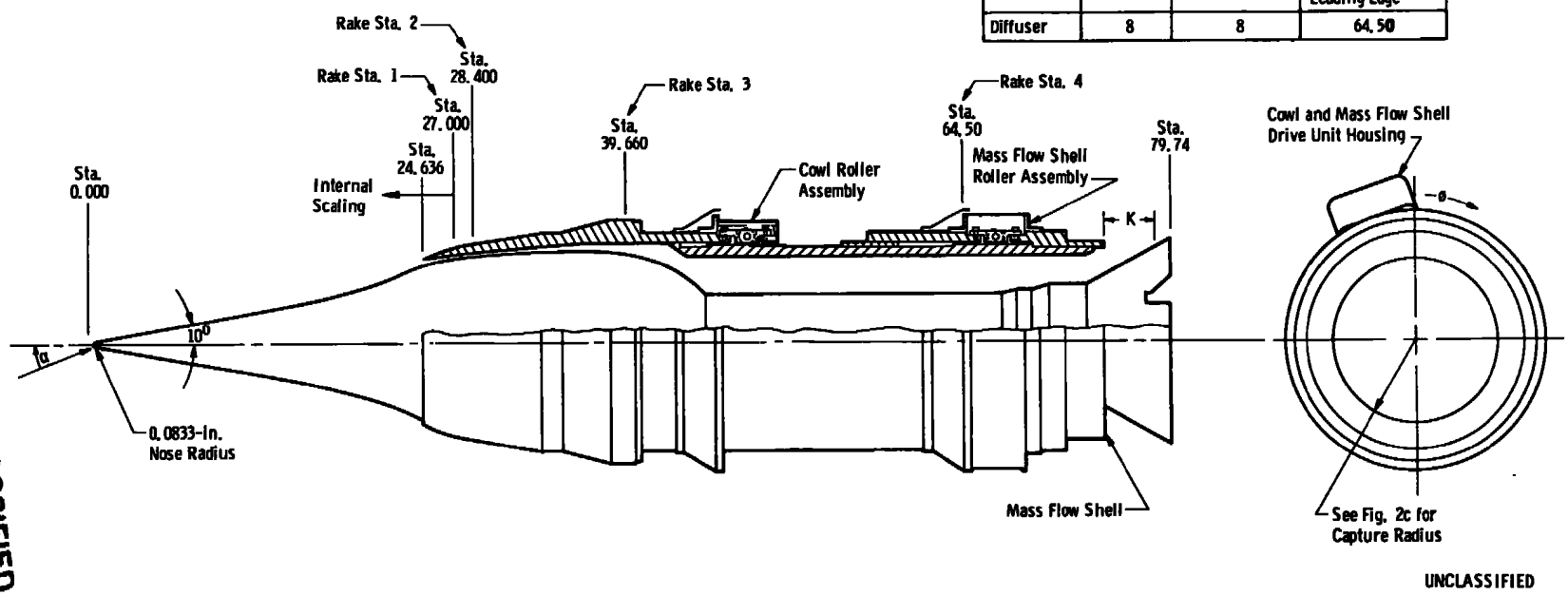

a. Model Assembly

Fig. 2 Model Assembly and Component Details

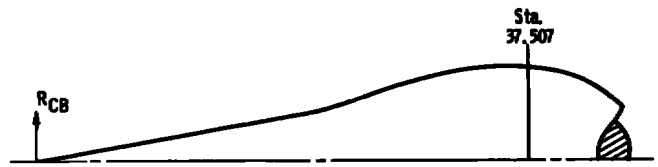

*Centerbody 1 (Final Configuration		Centerbody 2	
x, in.	R_{CB}, in.	x, in.	R_{CB}, in.
0.397	0	0.397	0
0.465	0.082	0.465	0.082
12.240	2.158	12.240	2.158
12.869	2.274	12.869	2.274
13.628	2.422	13.628	2.422
14.460	2.590	14.460	2.590
15.220	2.748	15.220	2.748
15.900	2.892	15.900	2.892
17.250	3.188	17.250	3.188
17.844	3.323	17.884	3.323
18.600	3.504	18.600	3.504
19.269	3.679	19.269	3.679
19.770	3.817	19.770	3.817
20.240	3.951	20.240	3.951
21.840	4.440	21.840	4.440
22.720	4.760	22.720	4.760
25.140	5.738	25.140	5.738
25.380	5.823	25.380	5.823
25.531	5.868	25.646	5.903
25.630	5.889	25.847	5.944
25.752	5.914	26.046	5.983
25.932	5.950	26.246	6.019
26.331	6.020	26.446	6.052
26.734	6.077	26.647	6.080
26.934	6.100	27.000	6.120
27.000	6.105	27.613	6.179
27.134	6.118	27.953	6.209
27.334	6.137	28.287	6.238
27.400	6.144	28.953	6.295
27.500	6.154	29.613	6.351
27.700	6.174	30.280	6.407
27.900	6.193	30.947	6.458
28.100	6.212	31.500	6.496
28.300	6.232	31.940	6.524
28.500	6.251	32.600	6.549
28.700	6.270	33.000	6.562
28.953	6.295	33.500	6.577
29.613	6.351	34.000	6.588
30.280	6.407	34.500	6.595
30.947	6.458	34.933	6.600
31.500	6.496	35.500	6.605
31.940	6.524	35.933	6.606
32.600	6.549	37.507	6.606
33.000	6.562		
33.500	6.577		
34.000	6.588		
34.500	6.595		
34.933	6.600		
35.500	6.605		
35.933	6.606		
37.507	6.606		

*Data Presented for this Configuration Only

CONFIDENTIAL

b. Centerbody Contours
Fig. 2 Continued

CONFIDENTIAL

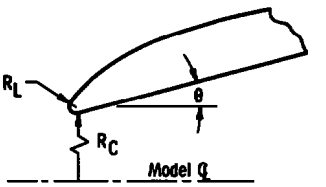

Leading-Edge Number	Leading-Edge Radius, R_L, in.	Capture Radius, R_C, in.	Inner Angle, θ, deg	Doubler Installed
1	0.020	5.976	16.40	No
2	0.020	5.985	13.25	No
3	0.020	6.000	12.00	No
4	0.040	6.000	12.00	Yes
5	$R_L \leq 0.002$	5.985	13.25	No
6	0.020	6.060	10.00	Yes
*7	0.020	6.000	12.00	Yes

*Final Configuration (Data Presented on this Configuration Only)

UNCLASSIFIED

c. Cowl Leading Edges

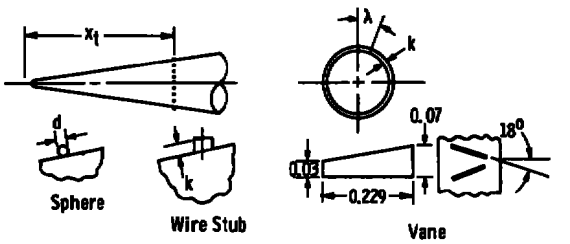

Trip Number	Position, x_t, in.	Roughness Shape	Spacing, λ, deg	Height, R, in.	Diameter, d, in.	+Mounting Band
*0	---	No Trips	---	---	---	---
1	4.66	Wire Stub	6.23	0.030	---	No
2	4.66	Sphere	6.55	0.031	0.031	No
3	4.66	Vane	9.00	See Above	---	No
4	4.66	No. 60 Grit	Random	0.017	---	No
5	8.00	Sphere	5.73	0.025	0.025	Yes
6	12.00	Sphere	2.43	0.015	0.015	Yes
7	20.00	Sphere	1.33	0.015	0.015	Yes
8	20.00	Sphere	2.75	0.031	0.031	Yes
9	20.00	Sphere	1.33	0.015	0.015	No

*Final Configuration (Data Presented on this Configuration Only)

+Nominal Mounting Band Thickness = 0.005 in.

UNCLASSIFIED

d. Centerbody Boundary-Layer Trips

Fig. 2 Continued

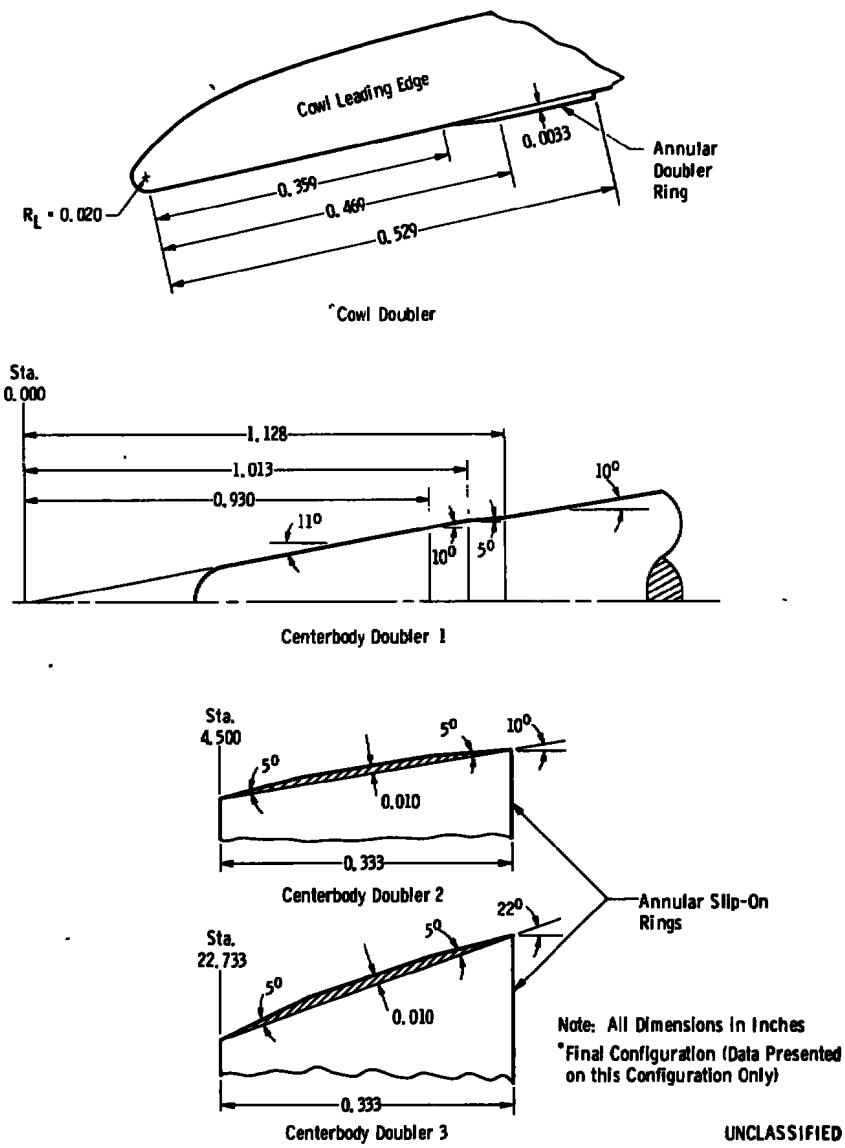

e. Doubler Bands

Fig. 2 Concluded

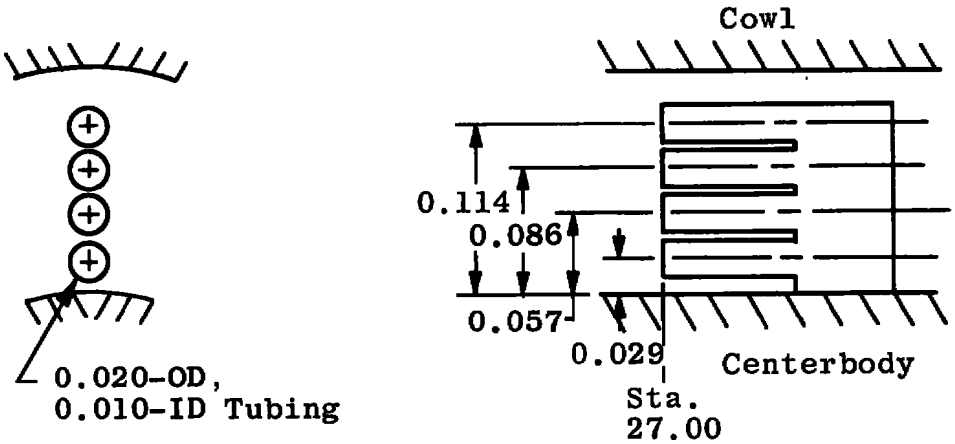

Rake Station 1

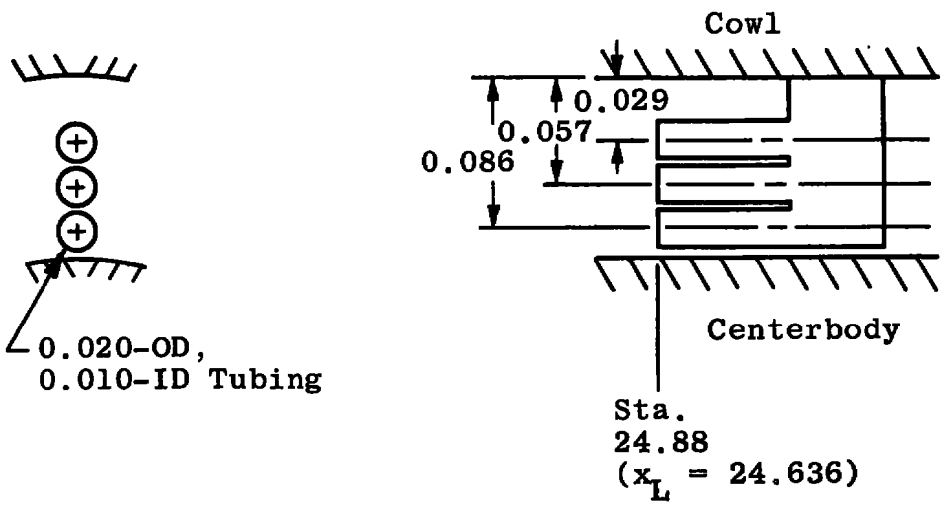

Rake Station 2

Note: Rakes at ϕ = 0 and 90 deg are identical.
All Dimensions in Inches

UNCLASSIFIED

a. Forward Throat Rakes for Stations 1 and 2

Fig. 3 Pitot Pressure and Total Temperature Rake Geometry

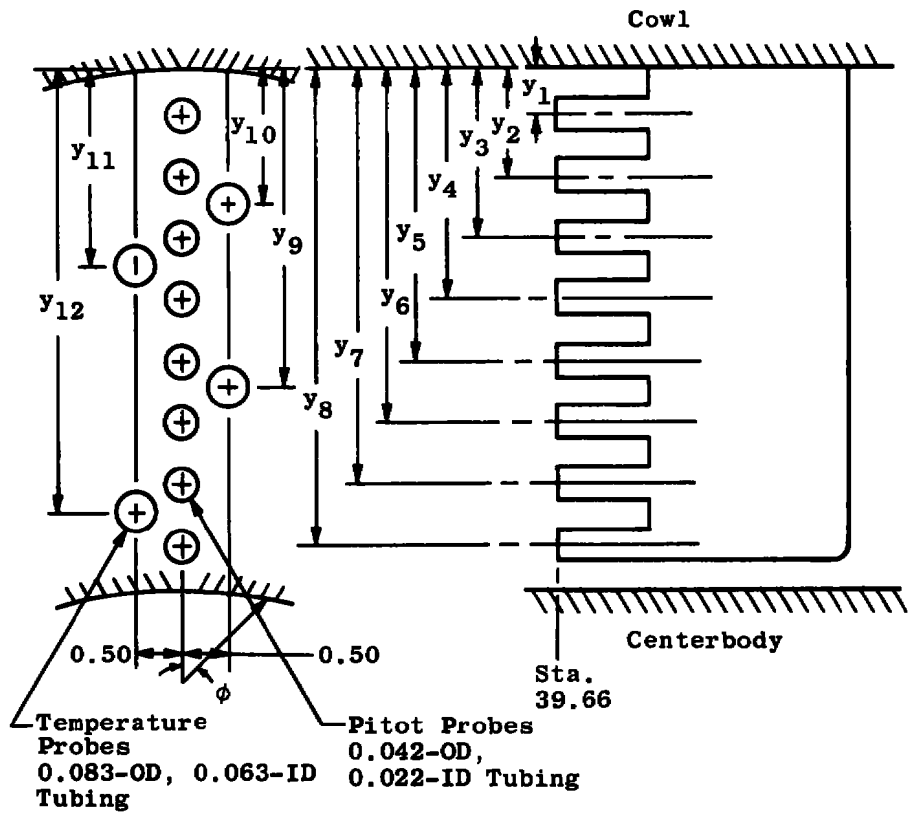

Note: Temperature probes omitted on side view for clarity.
All Dimensions in Inches

Rake 3		Rake 3A
ϕ	0	90 deg
y_1	0.0482	0.0282
y_2	0.0982	0.0982
y_3	0.1582	0.1482
y_4	0.2182	0.2082
y_5	0.2782	0.2682
y_6	0.3442	0.3182
y_7	0.4082	0.3882
y_8	0.4682	0.4582
y_9	0.2882	0.2982
y_{10}	0.1082	0.1382
y_{11}	0.2682	0.2382
y_{12}	0.4382	0.3982

UNCLASSIFIED

b. Diffuser Exit Rakes for Station 3
Fig. 3 Continued

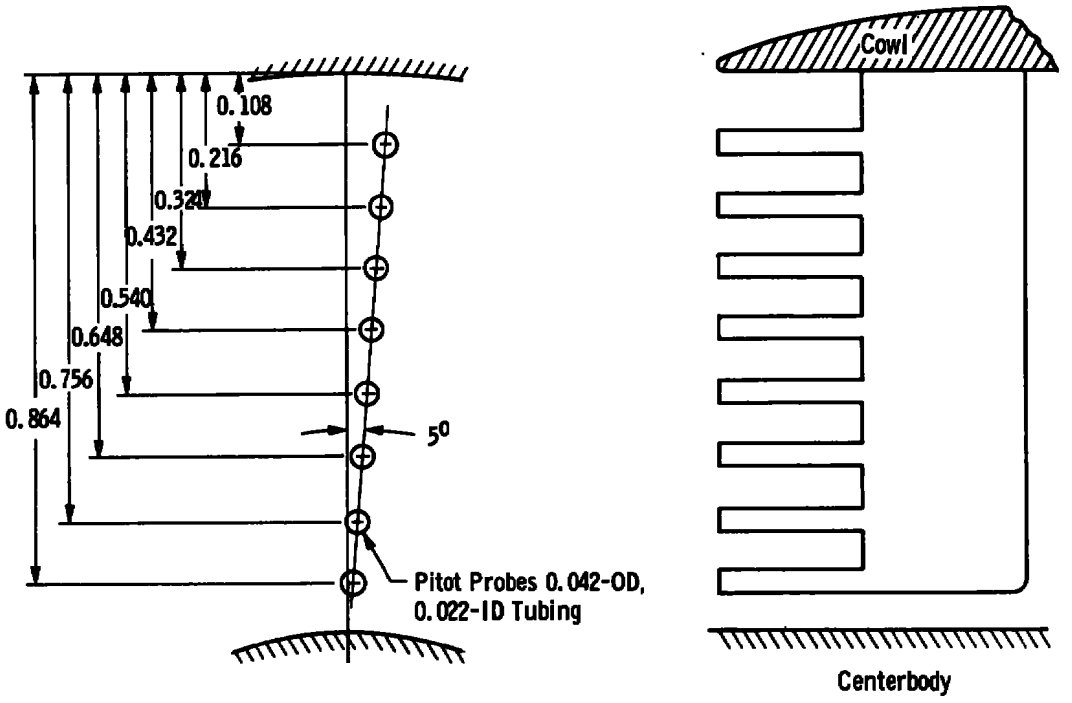

c. Spillage Drag Rake

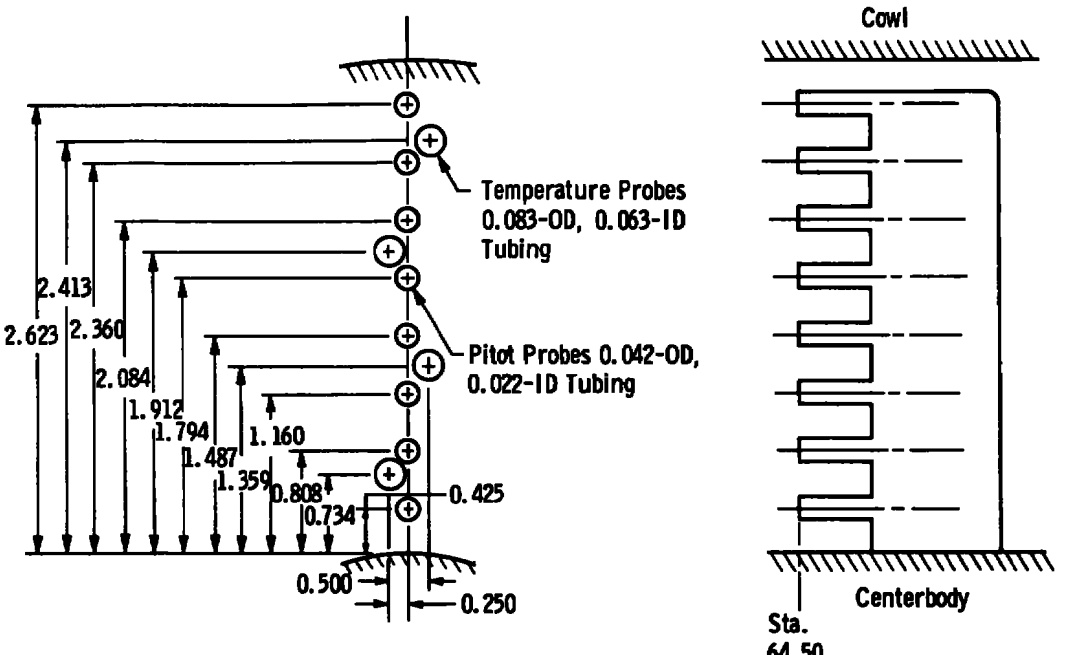

Note: Mass flow rakes located at ø = 45, 135, 225, and 315.
Temperature probes omitted on side view for clarity.
All Dimensions in Inches

UNCLASSIFIED

d. Mass Flow Rakes for Station 4

Fig. 3 Concluded

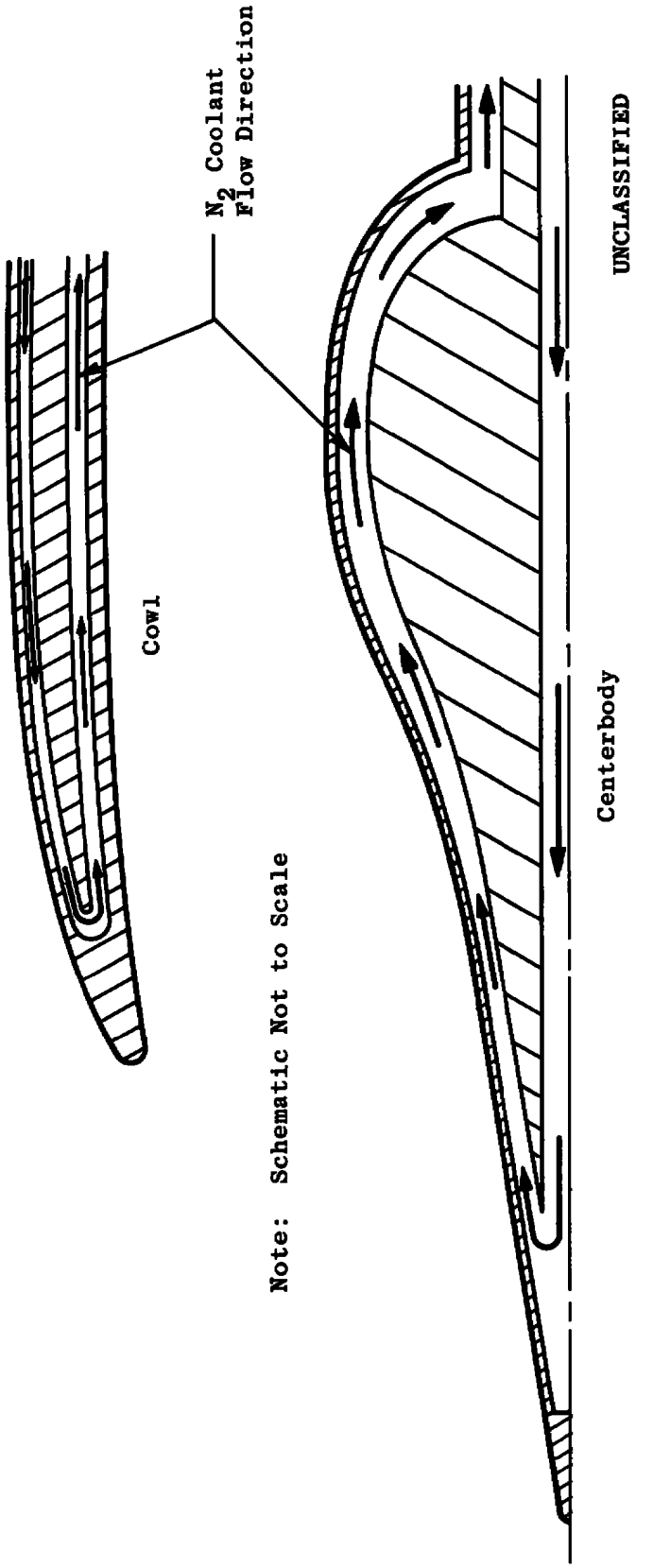

Fig. 4 Schematic of Model Cooling Passages

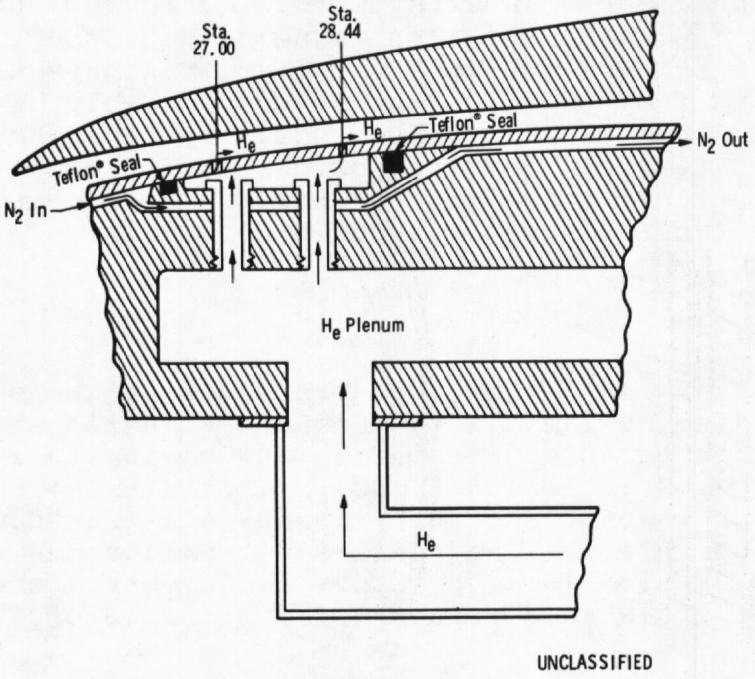

a. Schematic of Helium Injection System

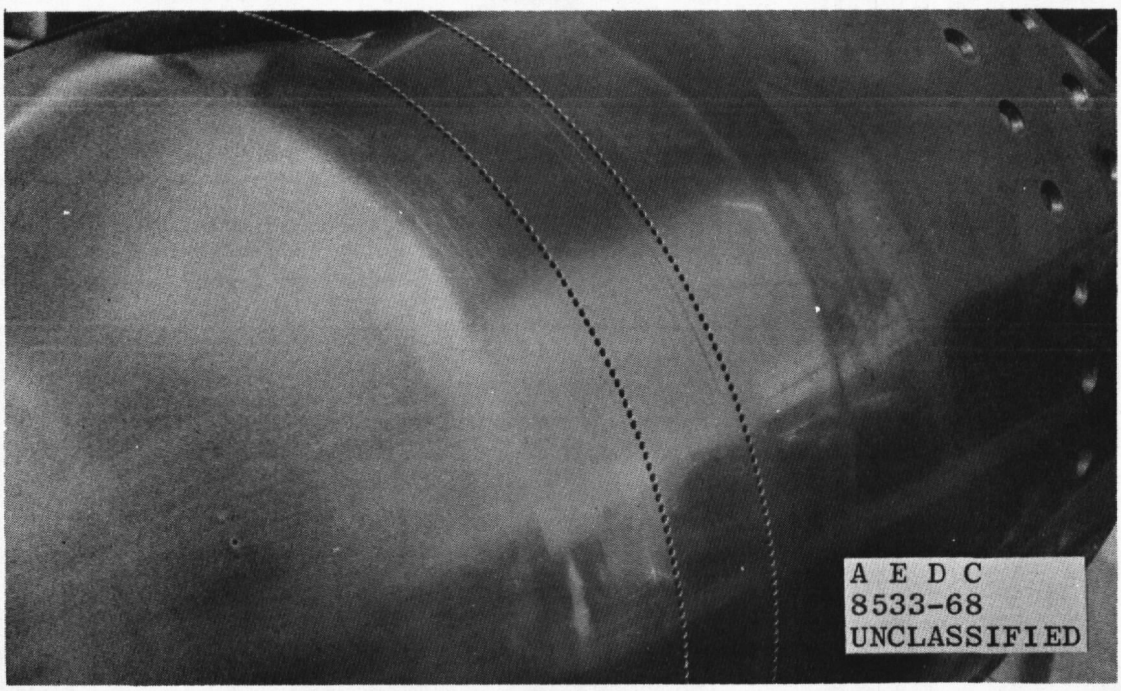

b. Photograph of Helium Injection Ports

Fig. 5 Schematic and Photograph of Helium Injection System

(U) Tunnel B has an axisymmetric contoured nozzle and a 50-in.-diam test section. The tunnel can be operated at a nominal Mach number of 6 or 8 at stagnation pressures from 20 to 300 and from 50 to 900 psia, respectively, at stagnation temperatures up to 1350°R. The model may be injected into the tunnel for a test run and then retracted for model changes without interrupting the tunnel flow. A more complete description of the tunnels may be found in Ref. 2.

2.3 INSTRUMENTATION

(U) In Tunnel A, the model pressures on the centerbody upstream of the cowl lip were measured with 15-psid transducers referenced to a near vacuum and having full-scale calibrated ranges of 15, 5, and 1 psi. The internal static and pitot pressures were measured with 60-psid transducers having a near-vacuum reference and full-scale calibrated ranges of 60, 20, and 4 psi. These pressure measurements are considered accurate to within ±0.3 percent of full scale of the range being used.

(U) Model pressures on the centerbody upstream of the lip station were also measured with 15-psid transducers in Tunnel B. The internal pressures were measured with 100- and 200-psid transducers, and all transducers were referenced to a near vacuum. From repeat calibrations, the estimated precision of the pressures measured with the 15-psid transducers was ±0.003 psia or ±0.5 percent, whichever was greater. The estimated precision of the measurements made with the 100- and 200-psid transducers was ±0.5 percent of full scale.

(U) Three strain-gage-type dynamic pressure transducers were installed in the walls of the duct. These transducers had a frequency response from 0 to 70 kilohertz and were designed for use over a pressure range from 1 to 50 psi. The dynamic transducer outputs were recorded on magnetic tape. The pressure data obtained from the dynamic pressure transducers will be analyzed by the Lockheed California Company. These data will serve as inputs for the engine structural and control design.

(U) Model Flow-field photographs were obtained during all tests. A typical photograph is shown in Fig. 6.

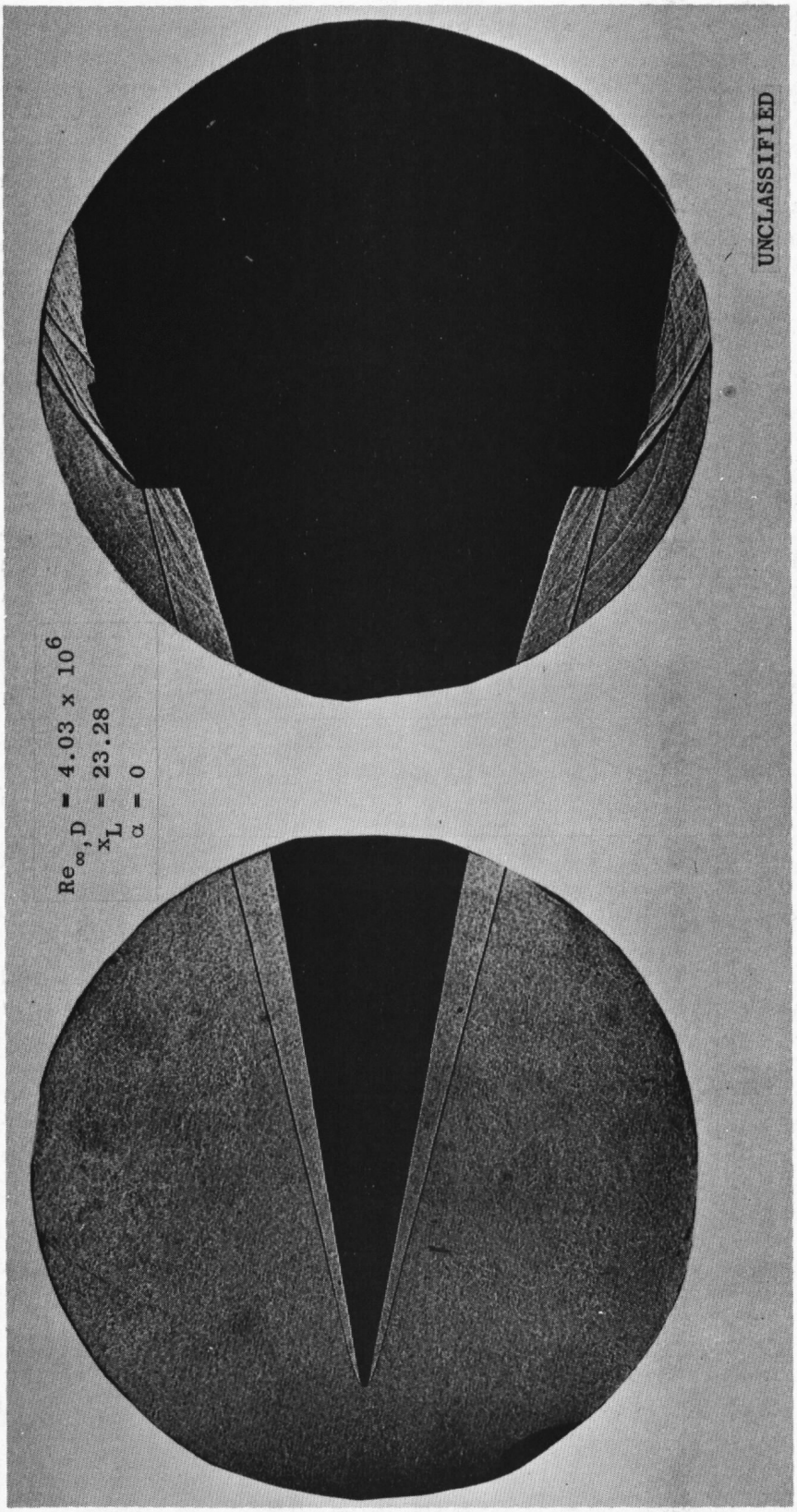

Fig. 6 Inlet Flow-Field Schlieren Photograph, Inlet Started, $M_\infty = 6.05$

SECTION III
PROCEDURE

3.1 TEST PROCEDURE

(U) The cowl was retracted near the close-off point while the tunnel was started (Tunnel A) or during model injection into the tunnel flow (Tunnel B). An approximate setting for the cooling system controls was made before the cowl was opened. The cowl was then moved forward to the test position, and the cooling was adjusted to a final setting. At Mach number 4, the wall temperature ratio, T_W/T_O, ranged from 0.55 on the forward centerbody to 0.85 near the cowl lip. The temperature range at Mach number 8 was from 0.15 to 0.75 over the same region. These were the minimum temperatures that could be maintained without heavy frost forming on the forward centerbody. If subsonic flow was desired at the station where mass flow rate was measured (rake station 4), the throttling shell was translated aft toward the closed position until the normal shock moved upstream of rake station 4.

(U) The first test objective was to determine the configurations which would start (that is, have supersonic flow through the inlet) at Mach number 4. Table I (Appendix) shows the various combinations of components tested. Only one configuration satisfied the Mach 4 start requirement. This configuration consisted on centerbody 1 and cowl lip 7 with the cowl doubler. A complete list of test conditions is presented in Table II (Appendix).

3.2 DATA REDUCTION

(U) Overall inlet total pressure recoveries and mass flows were computed from the pressure and temperature measurements. The following figure illustrates the geometric nomenclature of a typical rake station.

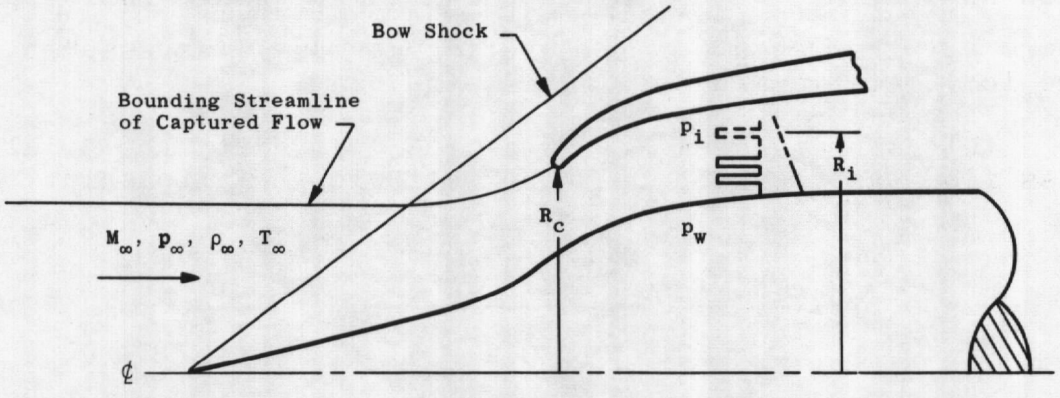

UNCLASSIFIED

Fig. 7 Typical Rake Station Geometry

(U) Pressure recoveries given herein were computed by mass-weighting the local pitot pressures and summing the elements across the duct. The expression used to accomplish this operation was

$$\eta_{\dot{m}} = \frac{1}{\dot{m}} \left[\sum_{i=1}^{n} \frac{\left[\frac{p_t}{p_o}\right]_i + \left[\frac{p_t}{p_o}\right]_{i+1}}{2} (\dot{m}_i) \right] \tag{1}$$

where $\dot{m}_i$ is the mass flow element at the i^{th} pitot position and $\dot{m}$ is the sum of i elements. The mass flow elements were calculated by

$$\frac{\dot{m}_i}{\dot{m}_\infty} = \frac{1}{2} \left\{ \left[\frac{\rho_s u}{\rho_\infty u_\infty}\right]_i + \left[\frac{\rho_s u}{\rho_\infty u_\infty}\right]_{i+1} \right\} \frac{R_{i+1}^2 - R_i^2}{R_c^2} \tag{2}$$

where the $\rho_s u$ terms were obtained from the following expression:

$$\left(\frac{\rho_s u}{\rho_\infty u_\infty}\right)_i = \frac{\left(\frac{p_{s_i}}{p_o}\right)}{\left(\frac{p_\infty}{p_o}\right)} \frac{M_i}{M_\infty} \left[\frac{\frac{T_\infty}{T_o}}{\frac{T_{s_i}}{T_{t_i}}} \frac{1}{\frac{T_{t_i}}{T_o}} \right]^{1/2} \tag{3}$$

The mass flow, $\dot{m}$, computed by this method was used only in the mass-weighting computations. The pressure and temperature ratios were computed from the isentropic flow relationships using 1.4 for the ratio of specific heats. The local Mach number, M_i, was obtained using the pressure ratio, p_{p_i}/p_w, where p_w (the measured wall static pressure) was assumed to be the local static pressure across the duct.

(U) Assuming choked flow at the duct exit, the total inlet mass flow was computed from the following relationship:

$$\frac{\dot{m}}{\dot{m}_\infty} = 0.5787 \frac{\bar{p}_R}{p_o} \frac{A_e}{A_c} \left[\frac{(1 + 0.2\ M_R^2)^{7/2}}{M_\infty (1 + 0.2\ M_\infty^2)^{-3}} \right] \sqrt{\frac{T_o}{T_{t_i}}} \tag{4}$$

where $\bar{p}_R$ is the average static pressure and $\bar{T}_{t_i}$ is the average measured total temperature at rake station 4. Temperature probe measurements were corrected as

$$\left(\frac{T_{t_i}}{T_o}\right)_{corrected} = \frac{T_{t_i}}{T_o} \frac{(1 + 0.2\ M_i^2)}{(1 + 0.2\, r\, M_i^2)} \tag{5}$$

where the recovery factor, r, was obtained by testing two total temperature probes at Mach number 10 to obtain the probe Reynolds number, Re_d, range expected during the test. This calibration is presented in Fig. 8. The total temperature probe corrections, as a function of Reynolds number based upon conditions upstream of the probe bow shock wave, was approximate since no consideration was given to differences in Mach number and total temperature levels.

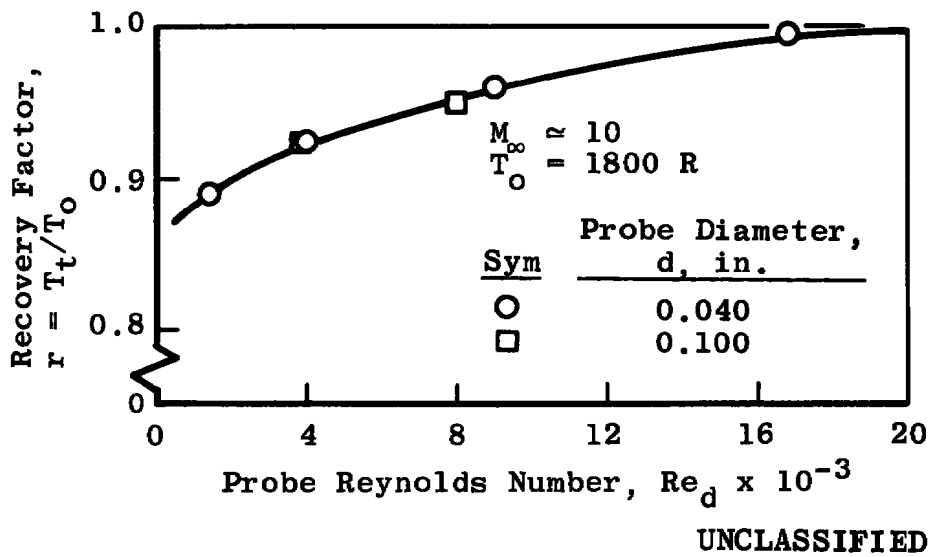

Fig. 8 Total Temperature Probe Recovery Factor

(U) The exit area, A_e, was obtained from the expression

$$A_e = 0.99\ (9.98 + 1339\ K + 1.443\ K^2 - 2.51\ K^3)10^{-4} \tag{6}$$

where K is shown in Fig. 2a. The rake station Mach number was obtained by iterating the following expression:

$$\frac{A_R}{A_e} = \frac{(1 + 0.2\ M_R^2)^3}{1.728} \tag{7}$$

(U) Spillage drag coefficients were calculated from

$$C_D = \frac{p_o/p_\infty}{0.7\ M_\infty^2} \left[\eta_A \frac{A_{stag}}{A_c} (1 + 0.2\ M_L^2)^{-7/2} (1 + 1.4\ M_L^2) \cos \theta_L \right.$$

$$\left. - \frac{\dot{m}}{\dot{m}_\infty} \frac{p_\infty}{p_o} (1 + 1.4\ M_\infty^2) + \frac{p_{CB}}{p_o} \frac{A_{stag}}{A_c} \right] \qquad (8)$$

where η_A is the area weighted pressure recovery at the cowl lip station. A discussion of spillage drag and a derivation of an expression equivalent to Eq. (8) is available in Ref. 3. Figure 9 illustrates the lip station geometric nomenclature used in Eq. (8).

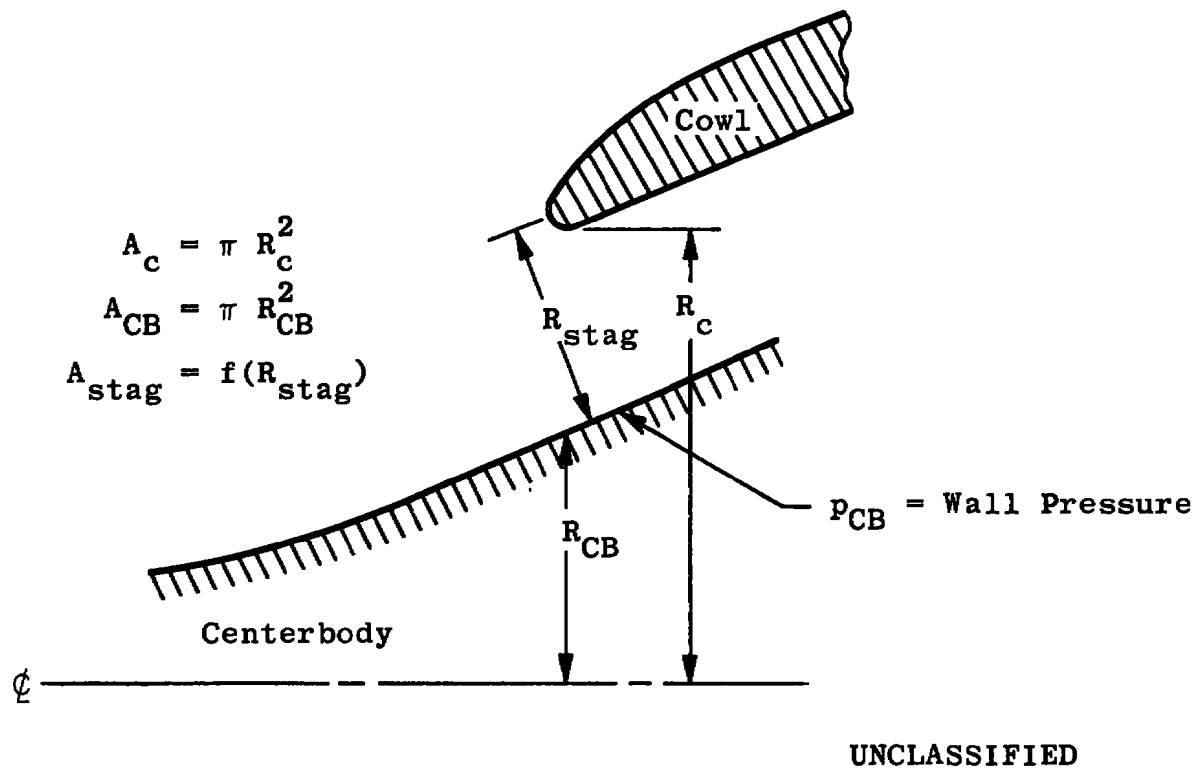

Fig. 9 Cowl Lip Station Geometry

SECTION IV
RESULTS AND DISCUSSION

(U) Representative data obtained on the final configuration of the two-thirds scale HRE inlet model are presented in this section. These data illustrate measurements along the centerbody and cowl at $\phi = 0$ and across the duct at rake stations 1, 2, and 3 ($\phi = 0$). Data obtained at Mach number 5 during the tests in Tunnel A are illustrated in Figs. 10 through 12. Varying the cowl position produced changes in the pressure and temperature distributions as shown in Fig. 10. The complex duct flow and resulting wave patterns are evidenced in the irregular pressure distributions on both the centerbody and cowl surfaces.

(U) The wall temperature distributions illustrated in Figs. 10a and b are presented to document the test conditions rather than to specify actual full-scale wall conditions. Cooling passage configurations and model materials were considerably different from the full-scale inlet (i.e., the model simulates the full-scale aerodynamic, but not the thermal configuration). Some of the irregularities in the wall temperature distributions presented may have been caused by nonuniform cooling rather than aerodynamic heat transfer.

(U) Pitot pressure and total temperature profiles at rake station 3 ($\phi = 0$), presented in Fig. 10c, indicate that reflected waves were attenuated upstream of this station. Consequently, rake station 3 pitot pressures varied smoothly as the duct contraction changed (i.e., as the cowl position varied).

(U) Figure 11 shows the effects of varying free-stream Reynolds number on the inlet pressure and temperature distributions. A small Reynolds number influence, probably caused by the lip shock-boundary layer interaction, was observed on the centerbody pressures near the cowl lip. The pitot pressure distribution at rake station 3, Fig. 11c, showed only a small variation with free-stream Reynolds number.

(U) The influence of angle of attack on pressure and temperature distributions is presented in Fig. 12. The level of the measured pressures and temperatures changed uniformly as the angle of attack was varied, and reasonably constant trends were maintained. The pitot pressure distribution at rake station 3, Fig. 12c, showed slight changes in level, but no significant profile distortion was evident.

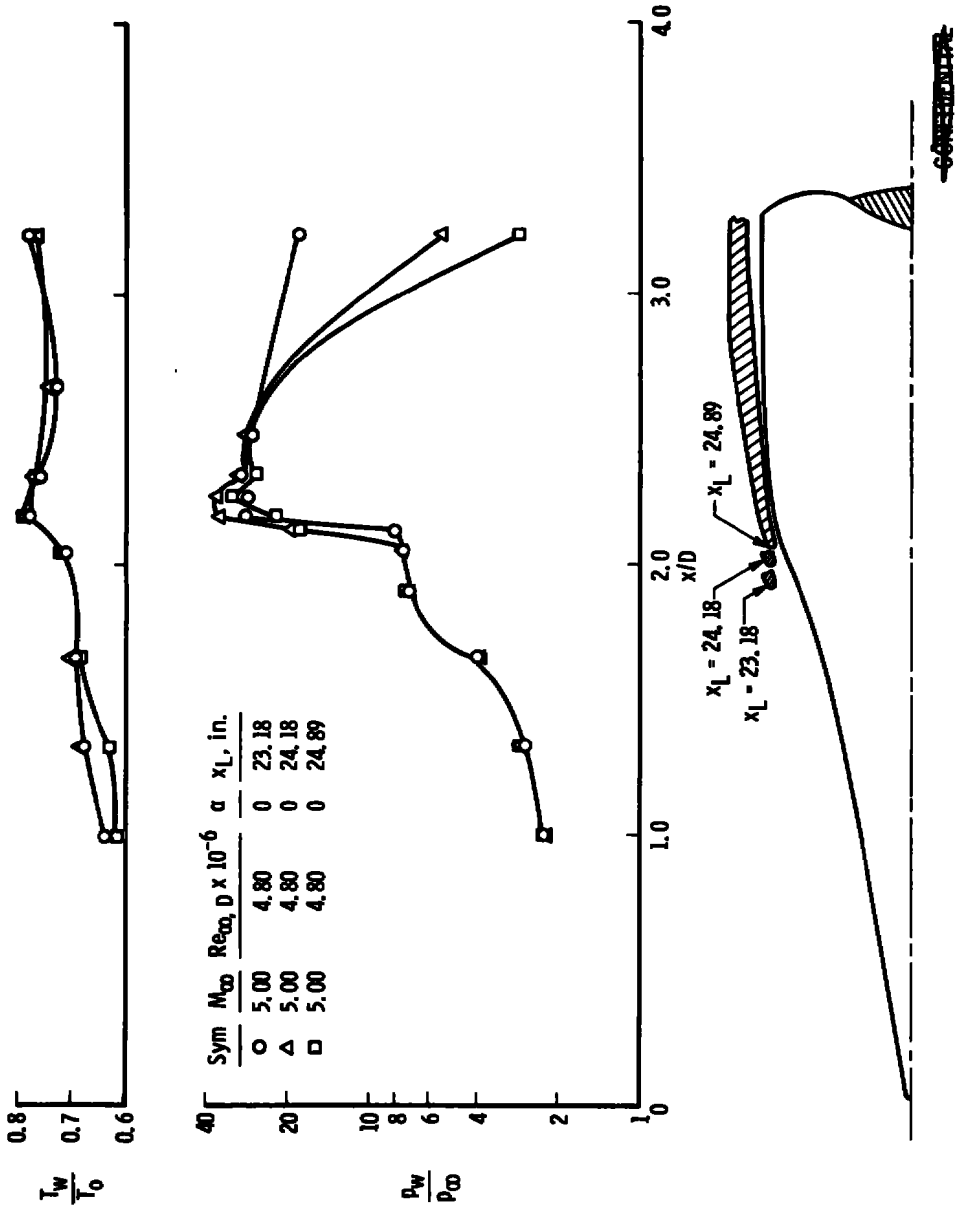

a. Centerbody Pressure and Temperature Distributions

Fig. 10 Effects of Cowl Position on Centerbody, Cowl, and Rake Station 3 Pressure and Temperature Distributions, M_∞ = 5.00

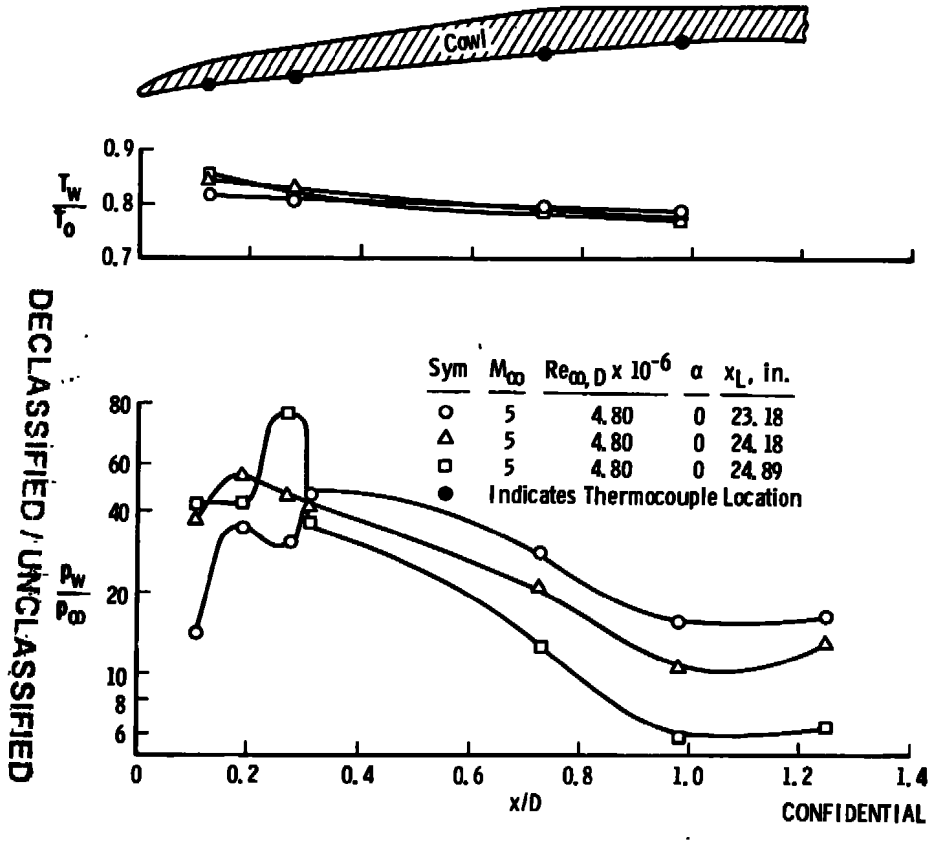

b. Cowl Pressure and Temperature Distributions

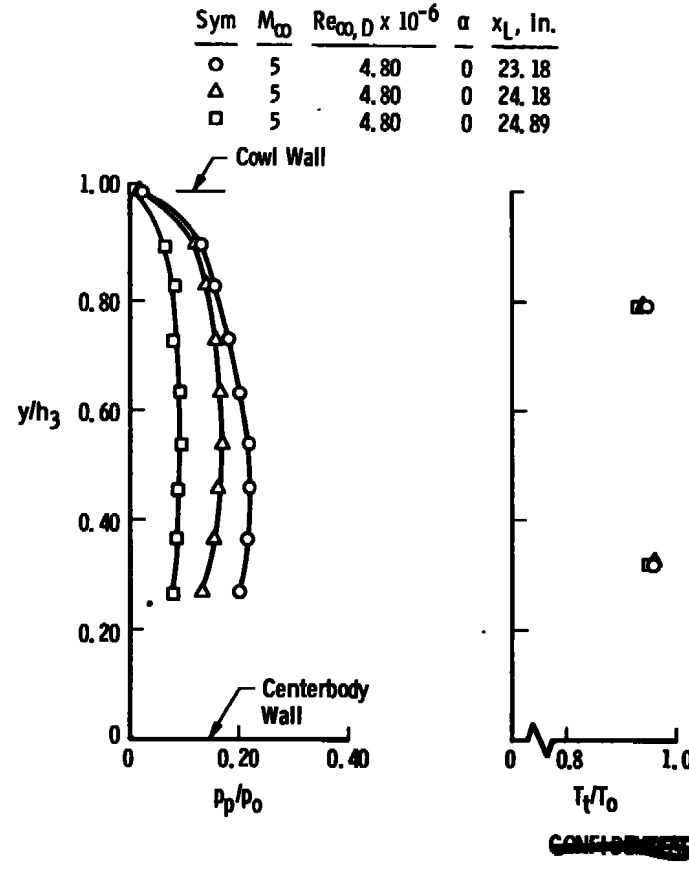

c. Rake Station 3 Pitot Pressure and Total Temperature Distributions

Fig. 10 Concluded

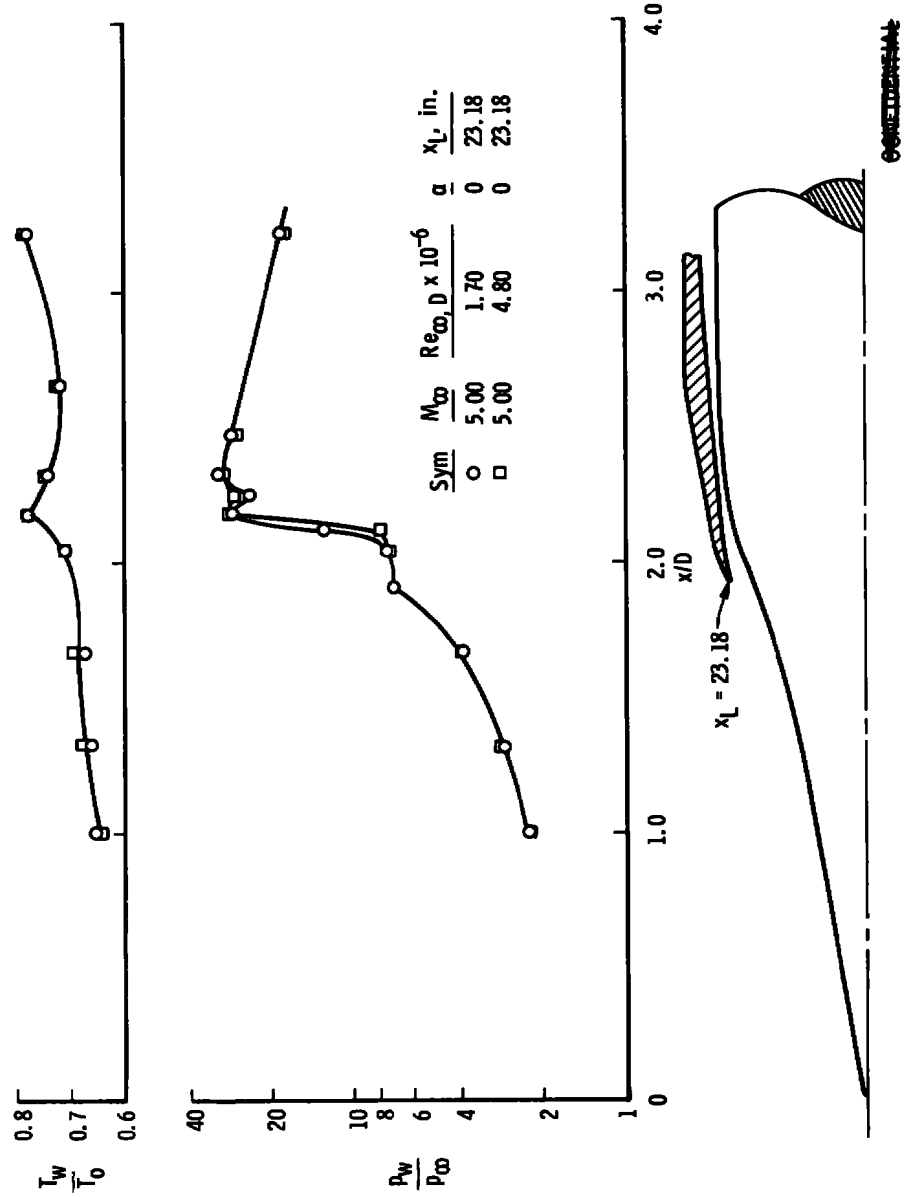

a. Centerbody Pressure and Temperature Distributions

Fig. 11 Effects of Reynolds Number on Centerbody, Cowl, and Rake Station 3 Pressure and Temperature Distributions, M_∞ = 5.00

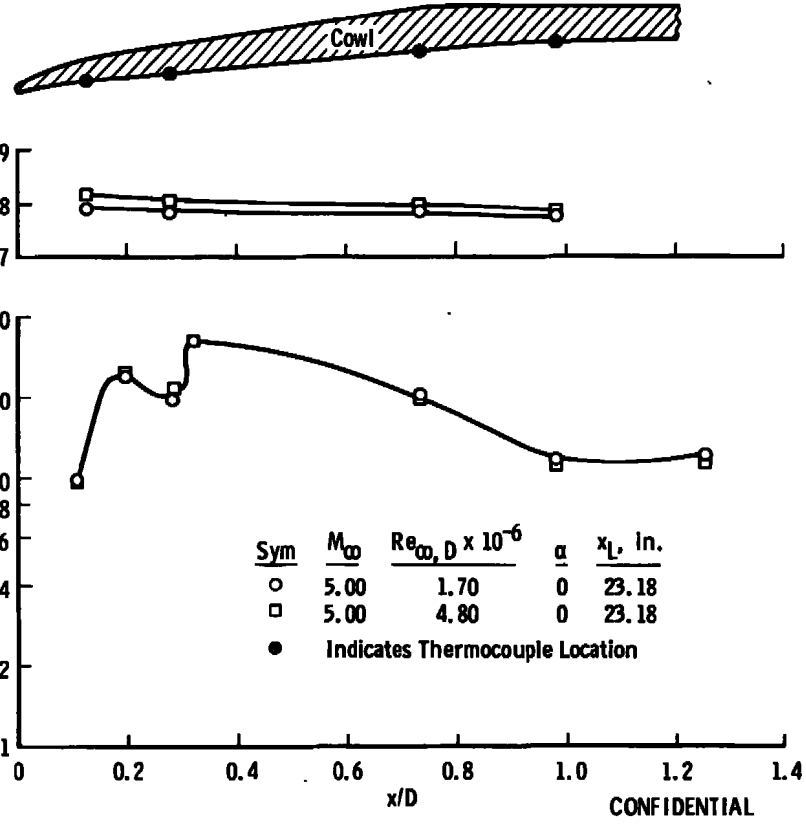

b. Cowl Pressure and Temperature Distributions

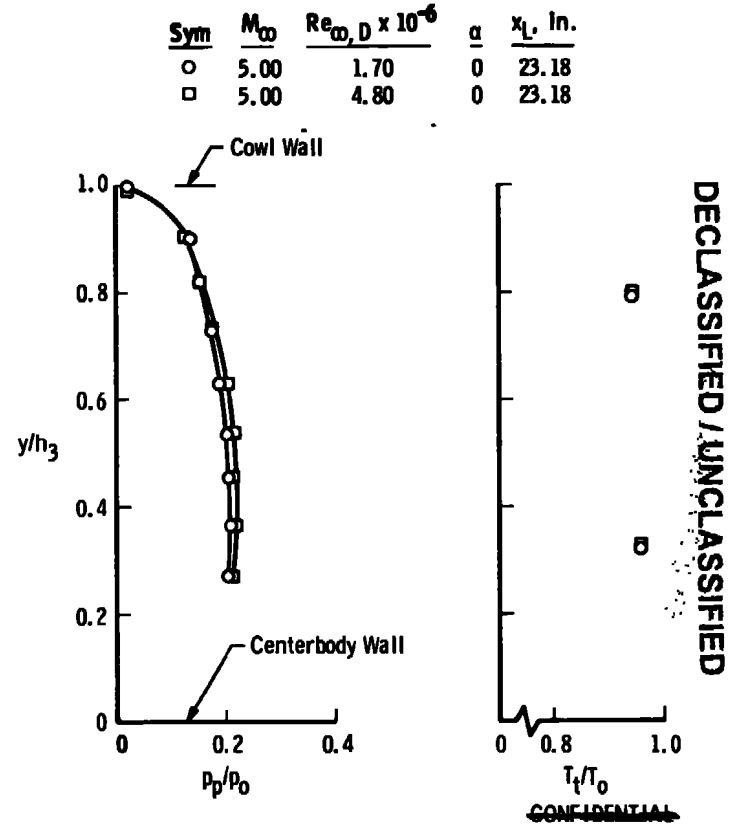

c. Rake Station 3 Pitot Pressure and Total Temperature Distributions

Fig. 11 Concluded

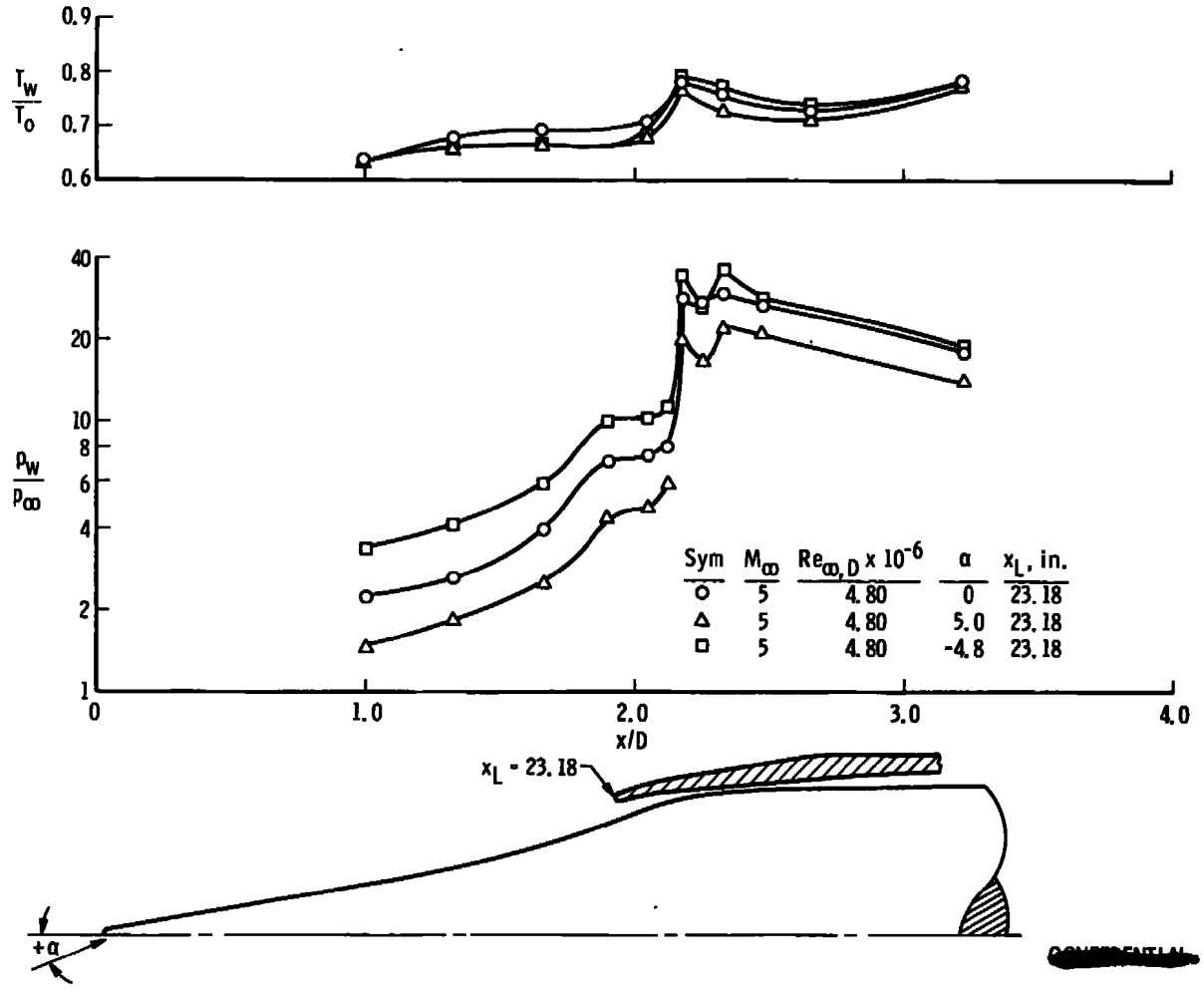

a. Centerbody Pressure and Temperature Distributions

Fig. 12 Effects of Angle of Attack on Centerbody, Cowl, and Rake Station 3 Pressure and Temperature Distributions, M_∞ = 5.00

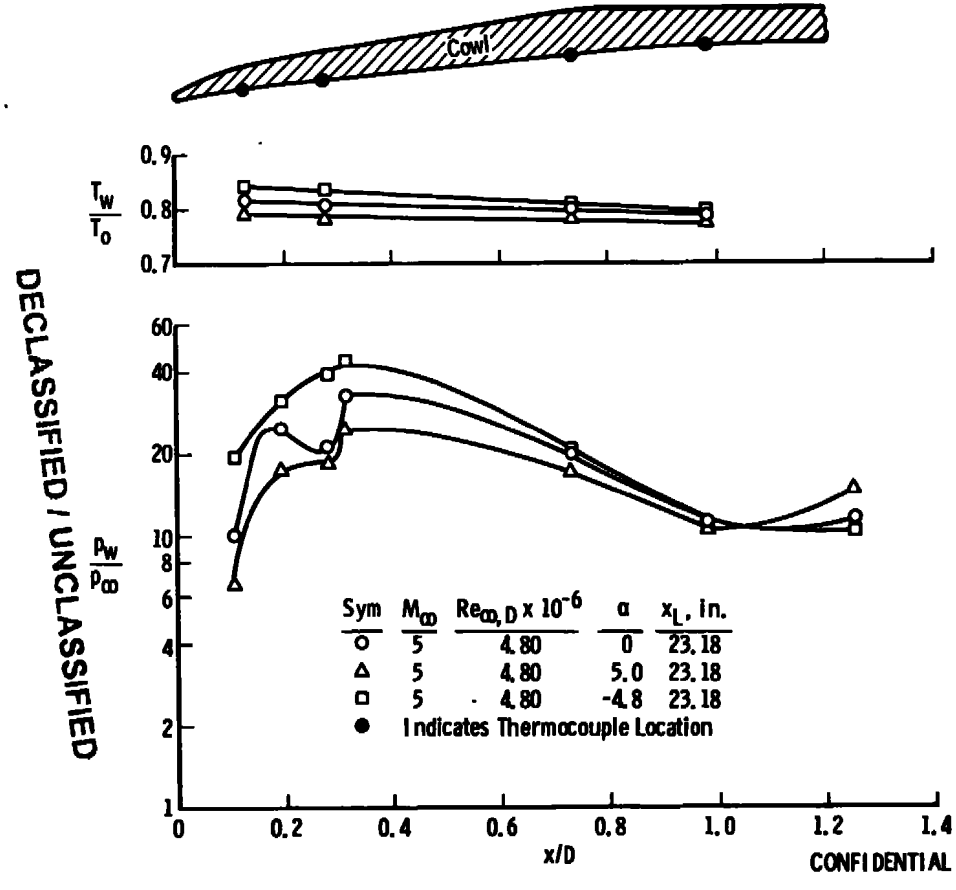

b. Cowl Pressure and Temperature Distributions

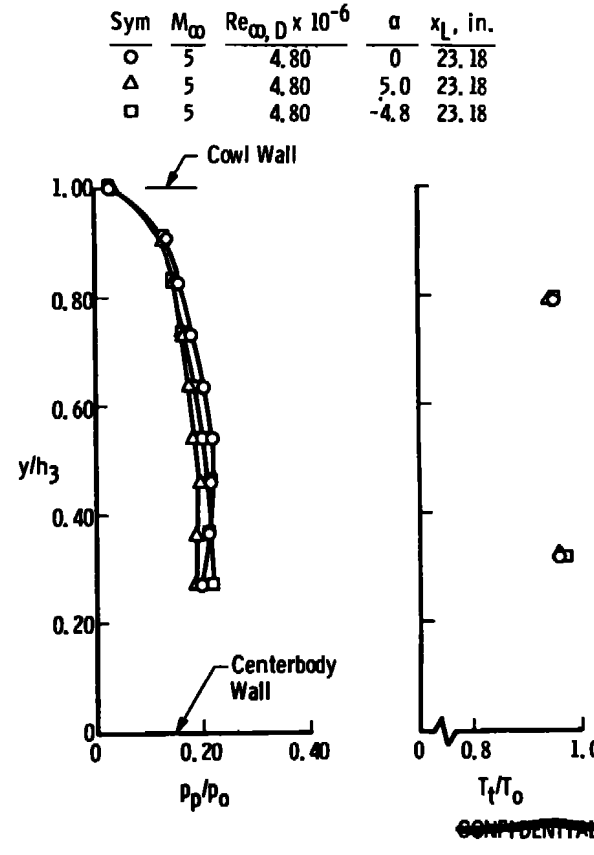

c. Rake Station 3 Pitot Pressure and Total Temperature Distributions

Fig. 12 Concluded

(U) Typical data obtained during the Mach 6 tests are shown in Figs. 13 through 15. These figures include pitot pressure distributions at rake stations 1 and 2. When the cowl was in the Mach 6 operating position (x_L = 23.26 in.), rakes 1 and 2 were spaced 0.10 in. apart axially; therefore, a combination of data from both rakes can be used as a reasonable approximation of the pitot pressure distribution across the entire duct. Figure 13 shows the effects of cowl position on the inlet pressure and temperature distributions. As in the Mach 5 data (Fig. 10), the irregular pressure distributions on the centerbody and cowl surfaces reveal the movement of the primary and reflected shock-boundary layer interactions. The sharp increase in the wall temperature ratio at x/D = 1.66 may be the result of internal cooling variations as previously discussed. More orderly variations can be seen in the pitot pressure and total temperature distributions in Fig. 13c. The largest changes were at rake station 1 which was nearest the cowl lip and in the region of reflected waves and duct flow development. The sensitivity of the flow in this area to cowl motion will be significant if, during supersonic burning, the zone of combustion moves upstream in the duct.

(U) Variations in pressure and temperature distributions at Mach number 6 caused by changes in the model angle of attack are presented in Fig. 14. The inlet would not remain started at 5 deg angle of attack; therefore, the ±3 deg data are shown. Perhaps the most significant data in this figure are the pitot pressure profiles at rake station 1. It appears that the total pressure recovery at this station decreases regardless of which direction the model pitched. These data again indicate the sensitivity of the forward throat region pressures to external changes.

(U) Variation in the inlet pressure and temperature distributions caused by changes in the free-stream Reynolds number are demonstrated in Fig. 15. Similar to the Mach number 5 data (Fig. 11), changes occurred near the cowl lip in the vicinity of the lip shock-boundary layer interaction and at rake station 1. There appears to have been a decrease in the profile distortion at this station while rake stations 2 and 3 showed no appreciable changes.

(U) A comparison of inlet pressure and temperature distributions over the Mach number range investigated is presented in Fig. 16. The data illustrated were obtained with the cowl in the operate or design position for each Mach number. These data were then converted to overall performance data which are shown in Fig. 17. The mass flow data were computed from Equation 4 using the wall pressures at rake station 4. These data reveal the discrepancies which result

from averaging discrete data points. Namely, the inlet bow shock was on or inside the cowl lip when the Mach number 6 and 8 data were recorded; therefore one would expect the mass flow ratio to be unity instead of the calculated 0.96. The rapid decrease in total pressure recovery at rake station 3 over the Mach 6 to 8 range is not highly significant. A change from subsonic to supersonic combustion is expected to take place at Mach number 6; therefore conditions at the more forward portion of the duct (rake station 1) are more significant.

(4) Data from the Mach number 3 spillage drag run at $\alpha = 0$ are shown in Fig. 18. Applying Equation 8 to these data yields $C_D = 0.54$. These data can be used to estimate, in part, the total aircraft-powerplant drag during low Mach number flight operations.

(5) The inlet remained started with helium (simulated fuel) injection even when the helium mass flow reached approximately 30 percent of the captured air mass flow. However, the actual mass flow of injected gas was in question by as much as 100 percent. This uncertainty resulted from leakage of gaseous nitrogen from the coolant passage by the Teflon® seals (Fig. 5) into the helium plenum.

(6) For the data presented in Figs. 10 through 17, the inlet flow was assumed symmetric when $\alpha = 0$. Consequently, only data from rakes 1, 2, and 3 ($\phi = 0$) were illustrated. There was, however, some flow distortion around the duct as evidenced by the comparisons of rake 3 and 3A pitot pressure profiles in Fig. 19. The difference between the profiles varied with cowl position and the largest variation occurred at the operating position. This profile distortion could have been caused by model asymmetries or small free-stream flow nonuniformities. The significance of these distortions has not been determined and is now being analyzed by the Lockheed California Company.

REFERENCES

1. Hube, Frederick K. "Tests of a One-Third Scale NASA Hypersonic Research Engine Inlet at Mach Numbers 6 and 8."(U) AEDC-TR-68-28, March 1968. (Confidential)

2. Test Facilities Handbook (Seventh Edition). "von Karman Gas Dynamics Facility, Vol. 4." Arnold Engineering Development Center, July 1968.

3. Sibulkin, Mervin. "Theoretical and Experimental Investigation of Additive Drag." NACA Report 1187, 1954.

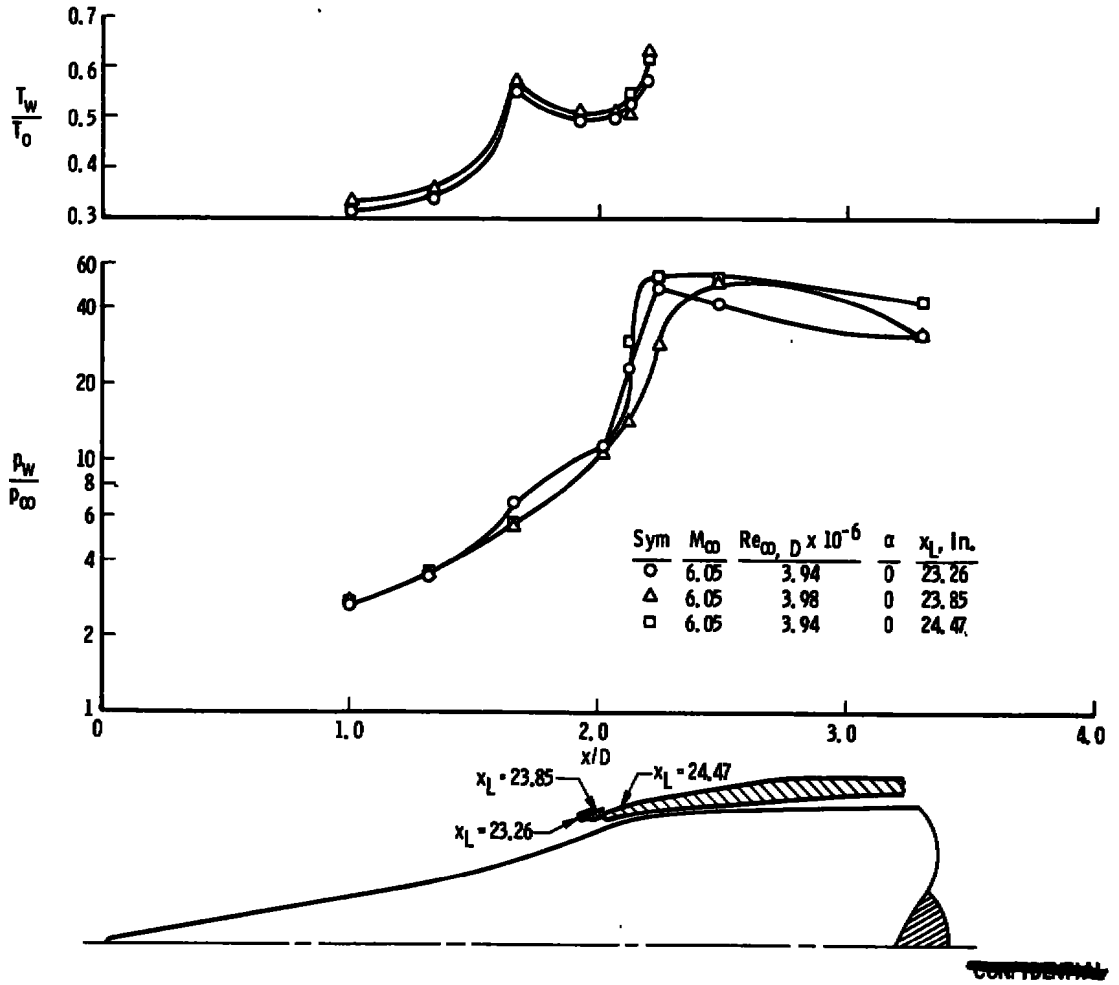

a. Centerbody Pressure and Temperature Distributions

Fig. 13 Effects of Cowl Position on Centerbody, Cowl, and Rake Pressure and Temperature Distributions, M_∞ = 6.05

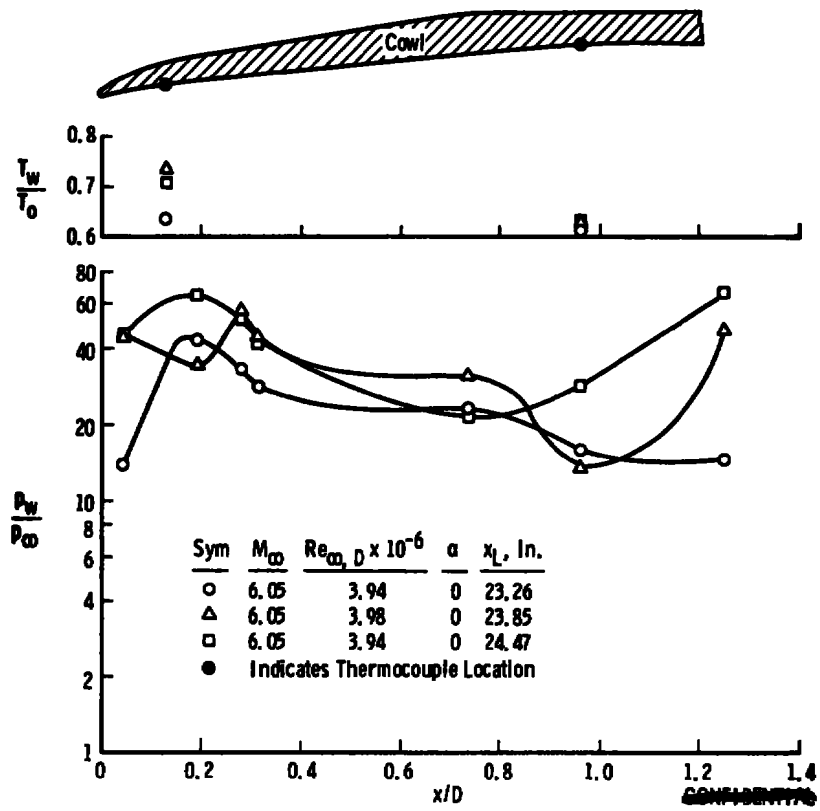

b. Cowl Pressure and Temperature Distributions
Fig. 13 Continued

Sym	M_∞	$Re_{\infty, D} \times 10^{-6}$	α	x_L, in.
○	6.05	3.94	0	23.26
△	6.05	3.98	0	23.85
□	6.05	3.94	0	24.47

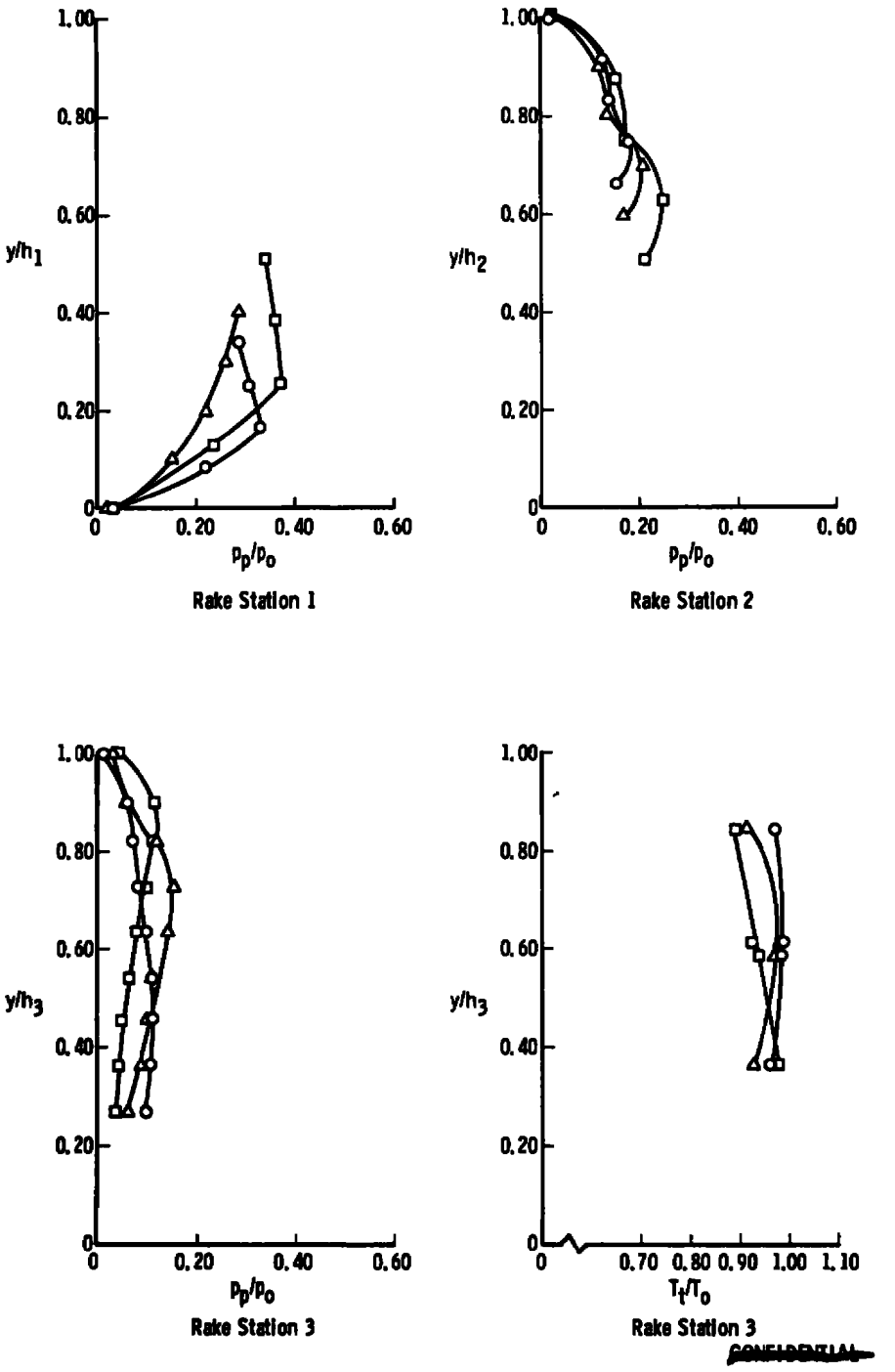

c. Rake Station Pitot Pressure and Total Temperature Profiles
Fig. 13 Concluded

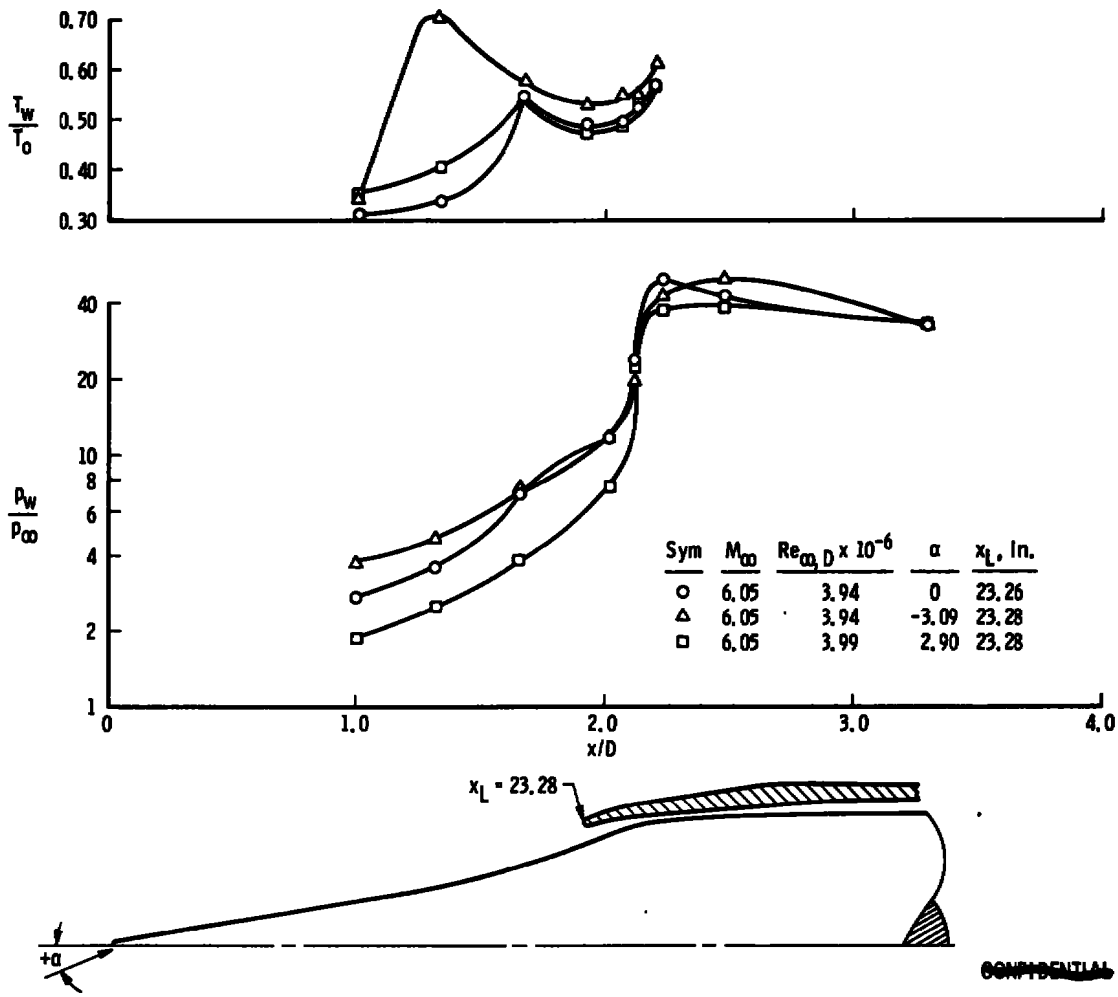

a. Centerbody Pressure and Temperature Distributions

Fig. 14 Effects of Angle of Attack on Centerbody, Cowl, and Rake Station Pressure and Temperature Distributions, M_∞ = 6.05

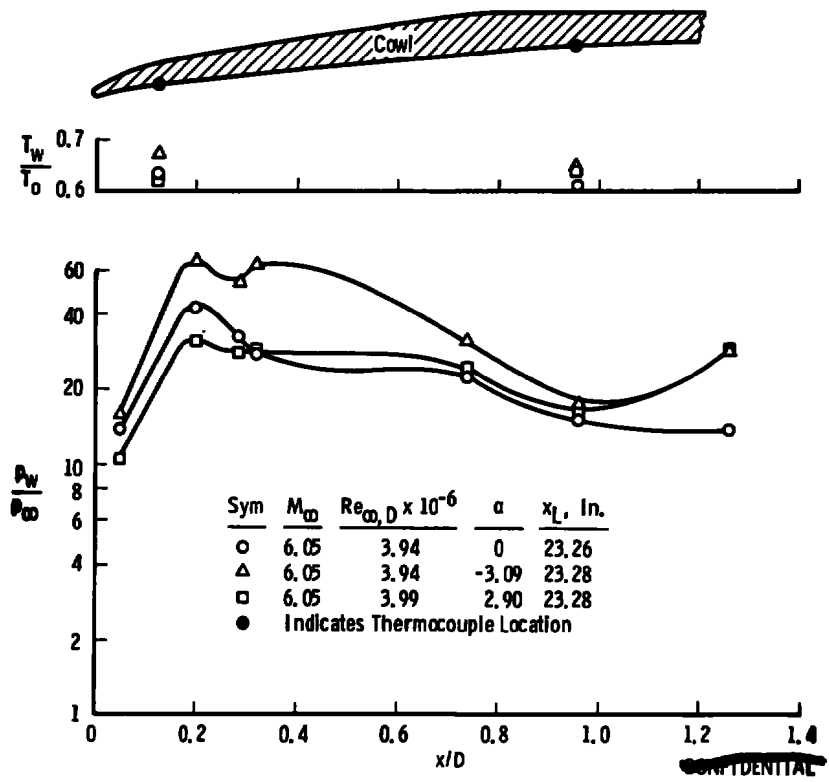

b. Cowl Pressure and Temperature Distributions
Fig. 14 Continued

Sym	M_∞	$Re_{\infty,D} \times 10^{-6}$	α	x_L, in.
○	6.05	3.94	0	23.26
△	6.05	3.94	-3.09	23.28
□	6.05	3.94	2.90	23.28

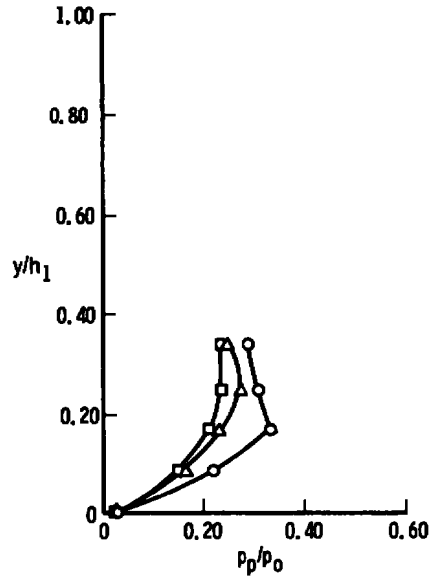

Rake Station 1

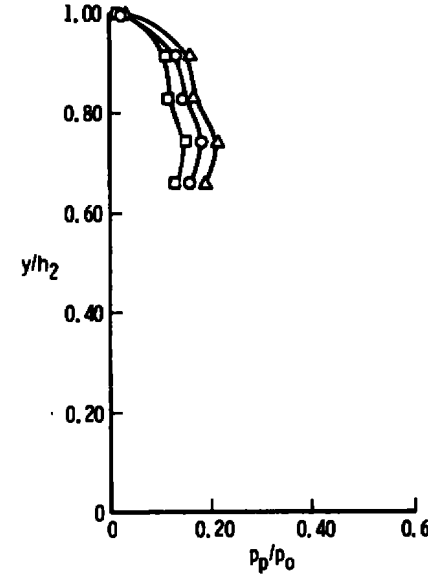

Rake Station 2

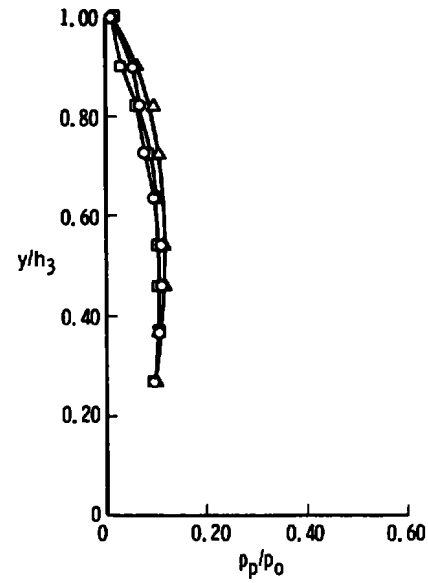

Rake Station 3

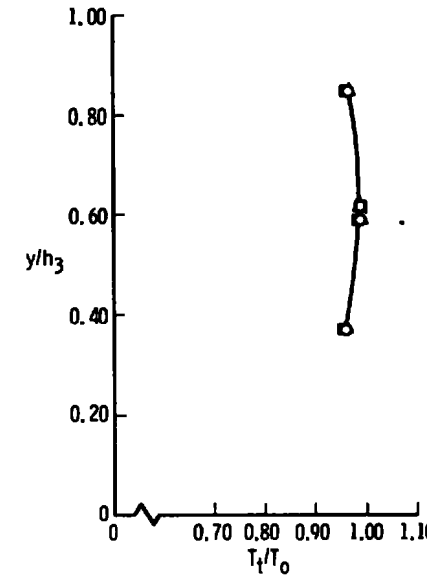

Rake Station 3

c. Rake Station Pressure and Temperature Distributions
Fig. 14 Concluded

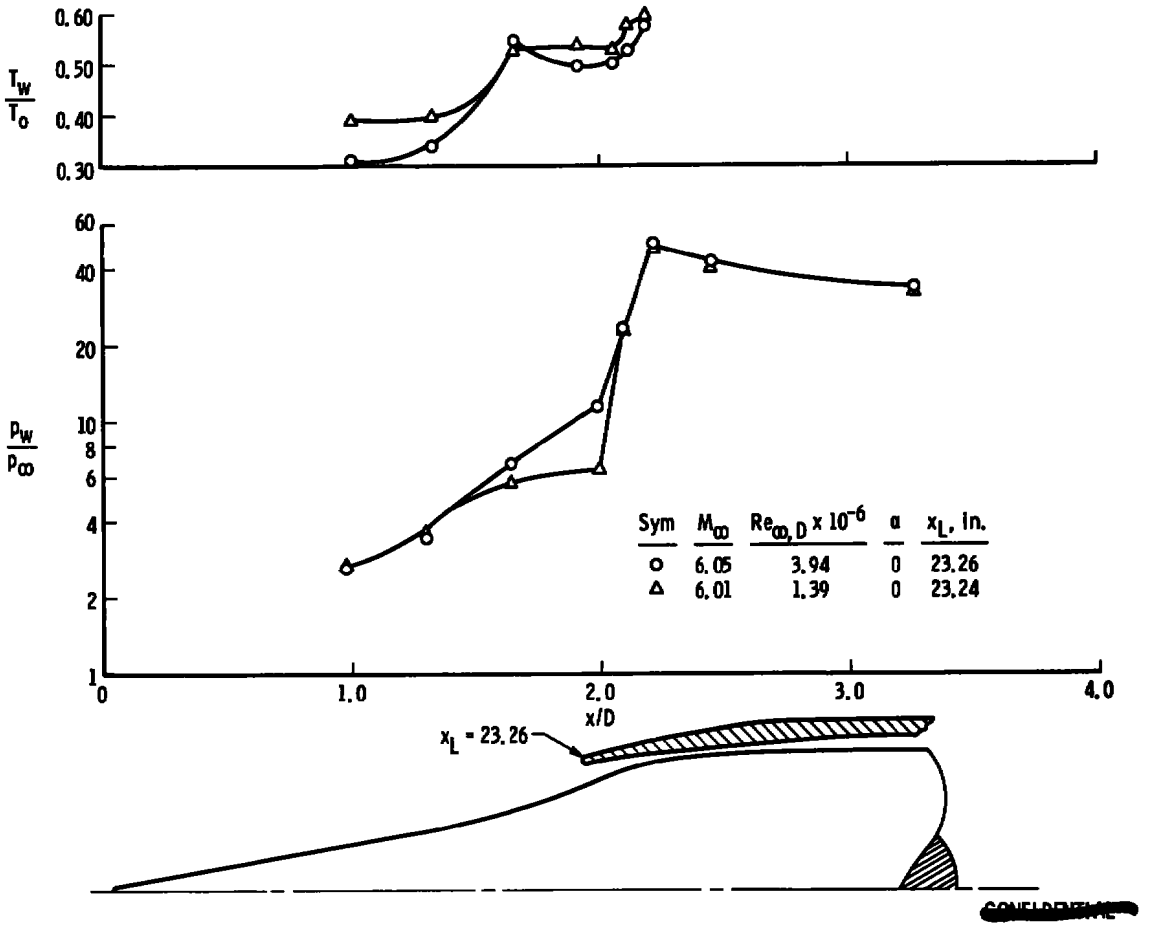

a. Centerbody Pressure and Temperature Distributions

Fig. 15 Effects of Reynolds Number on Centerbody, Cowl, and Rake Station Pressure and Temperature Distributions, M_∞ = 6

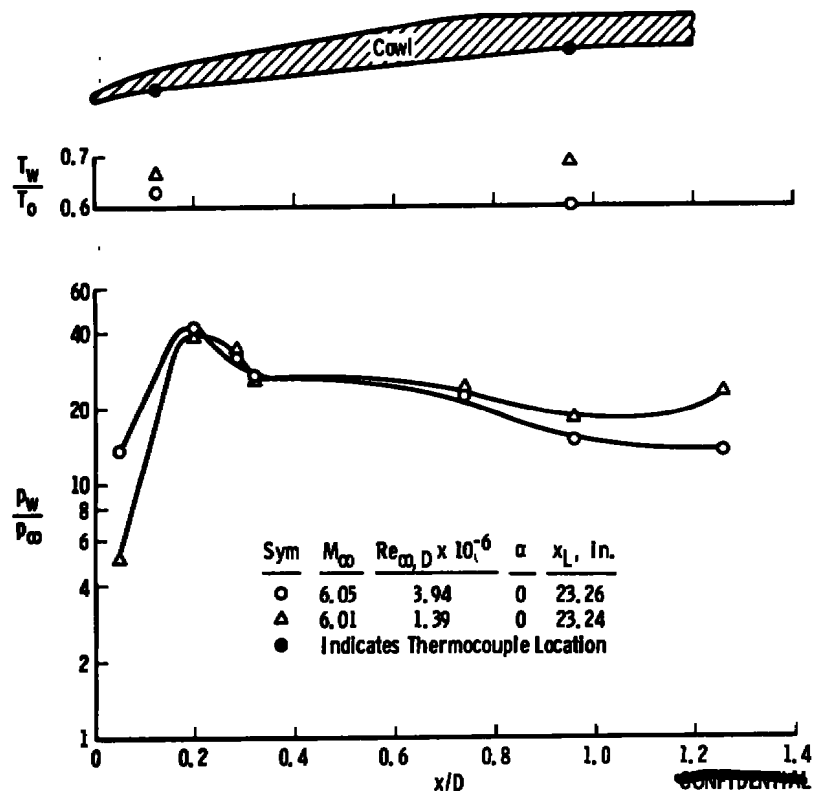

b. Cowl Pressure and Temperature Distributions
Fig. 15 Continued

Sym	M_∞	$Re_{\infty,D} \times 10^{-6}$	α	x_L, in.
○	6.05	3.94	0	23.26
△	6.01	1.39	0	23.24

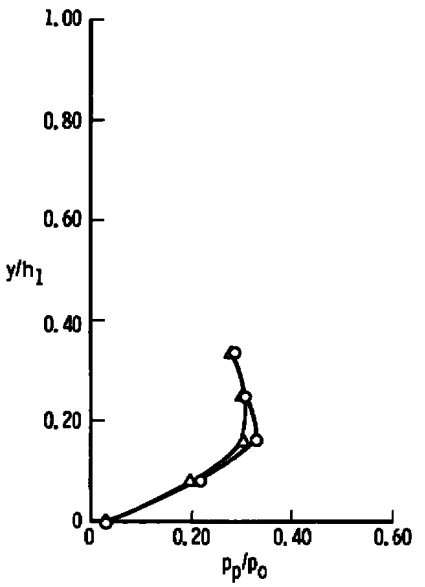

Rake Station 1

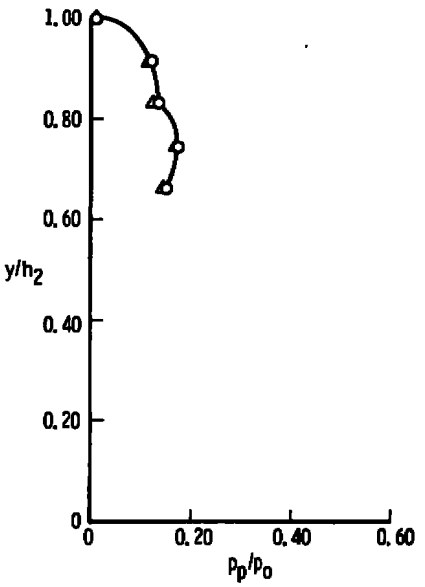

Rake Station 2

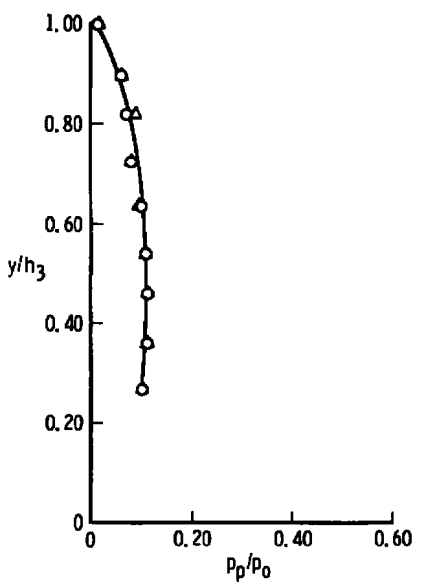

Rake Station 3

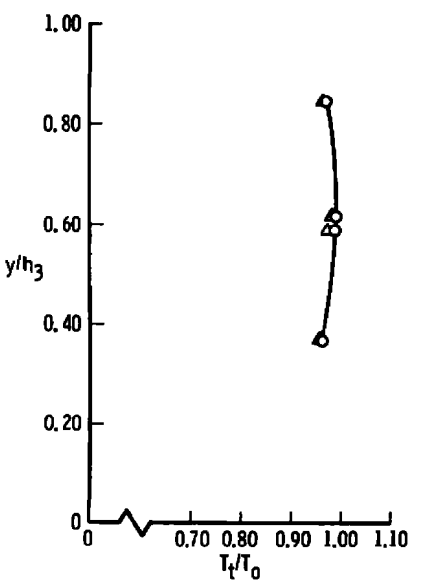

Rake Station 3

c. Rake Station Pitot Pressure and Total Temperature Distributions

Fig. 15 Concluded

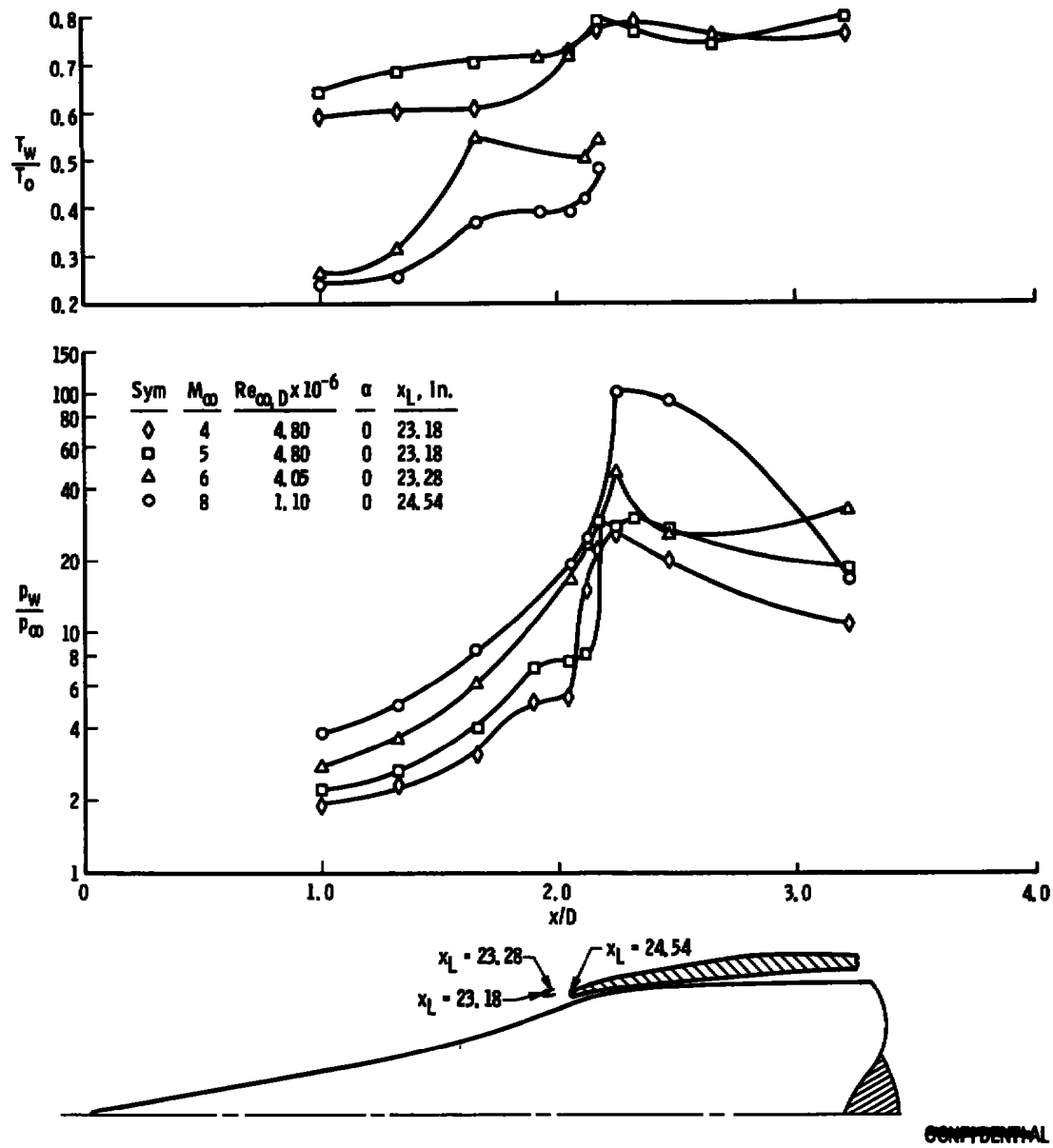

a. Centerbody Pressure and Temperature Distributions

Fig. 16 Comparison of Centerbody, Cowl, and Rake Station Pressure and Temperature Distributions at the Operating Cowl Position

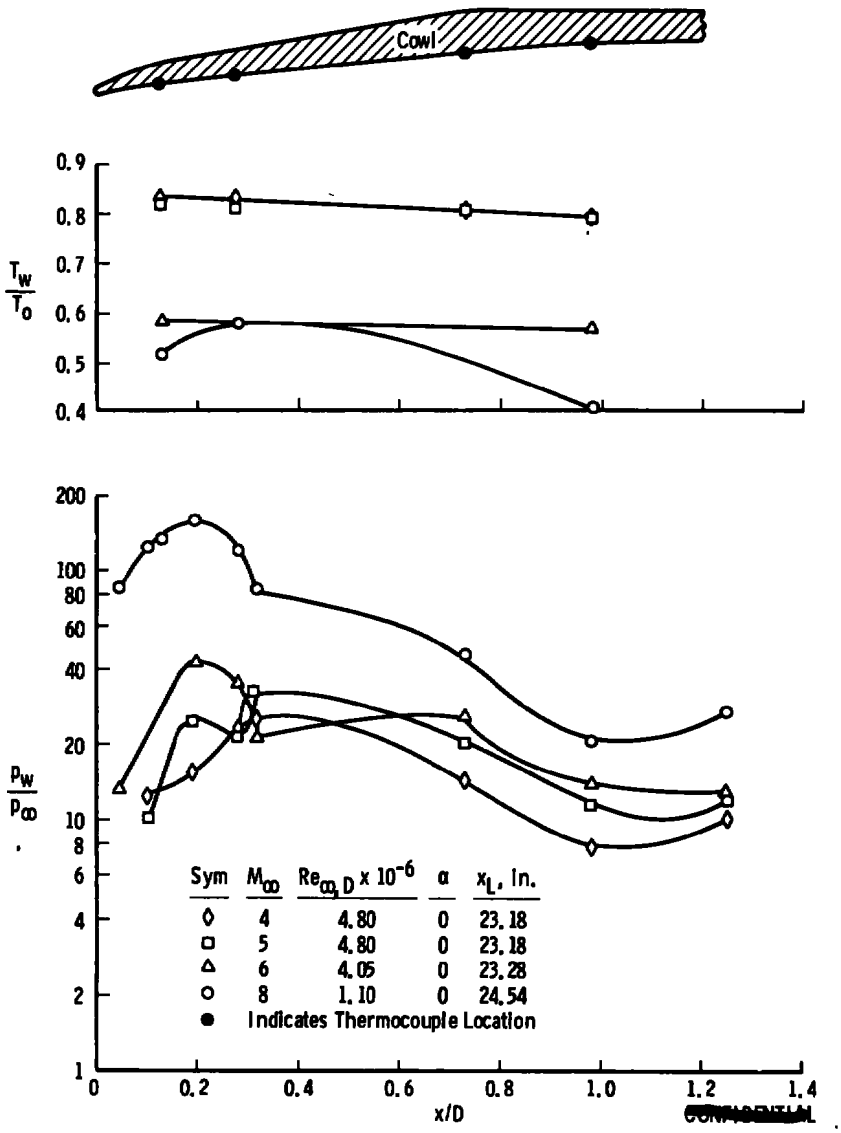

b. Cowl Pressure and Temperature Distributions
Fig. 16 Continued

Sym	M_∞	$Re_{\infty,D} \times 10^{-6}$	α	x_L, in.
◇	4	4.80	0	23.18
□	5	4.80	0	23.18
△	6	4.05	0	23.28
○	8	1.10	0	24.54

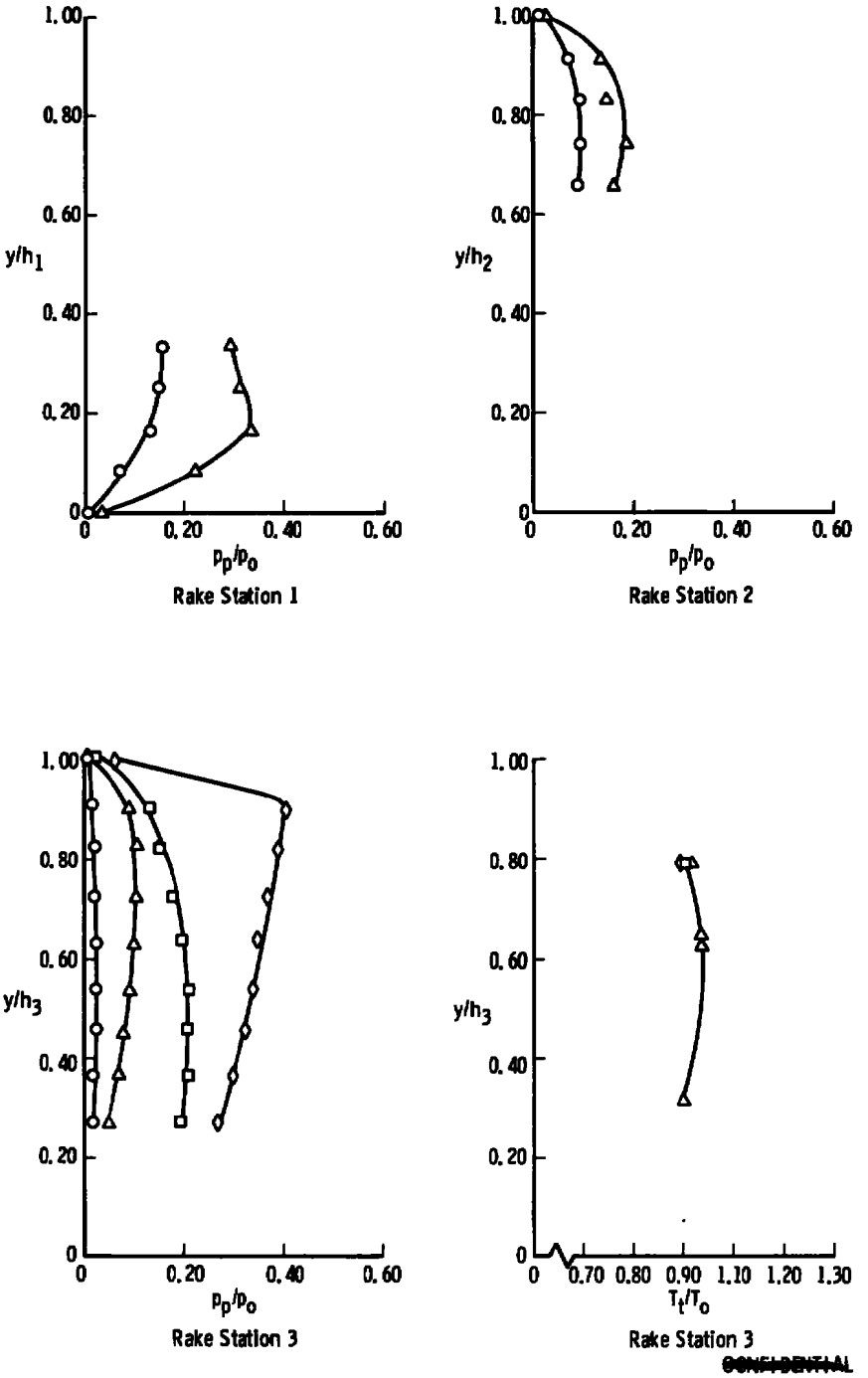

c. Rake Station Pitot Pressure and Total Temperature Distributions
Fig. 16 Concluded

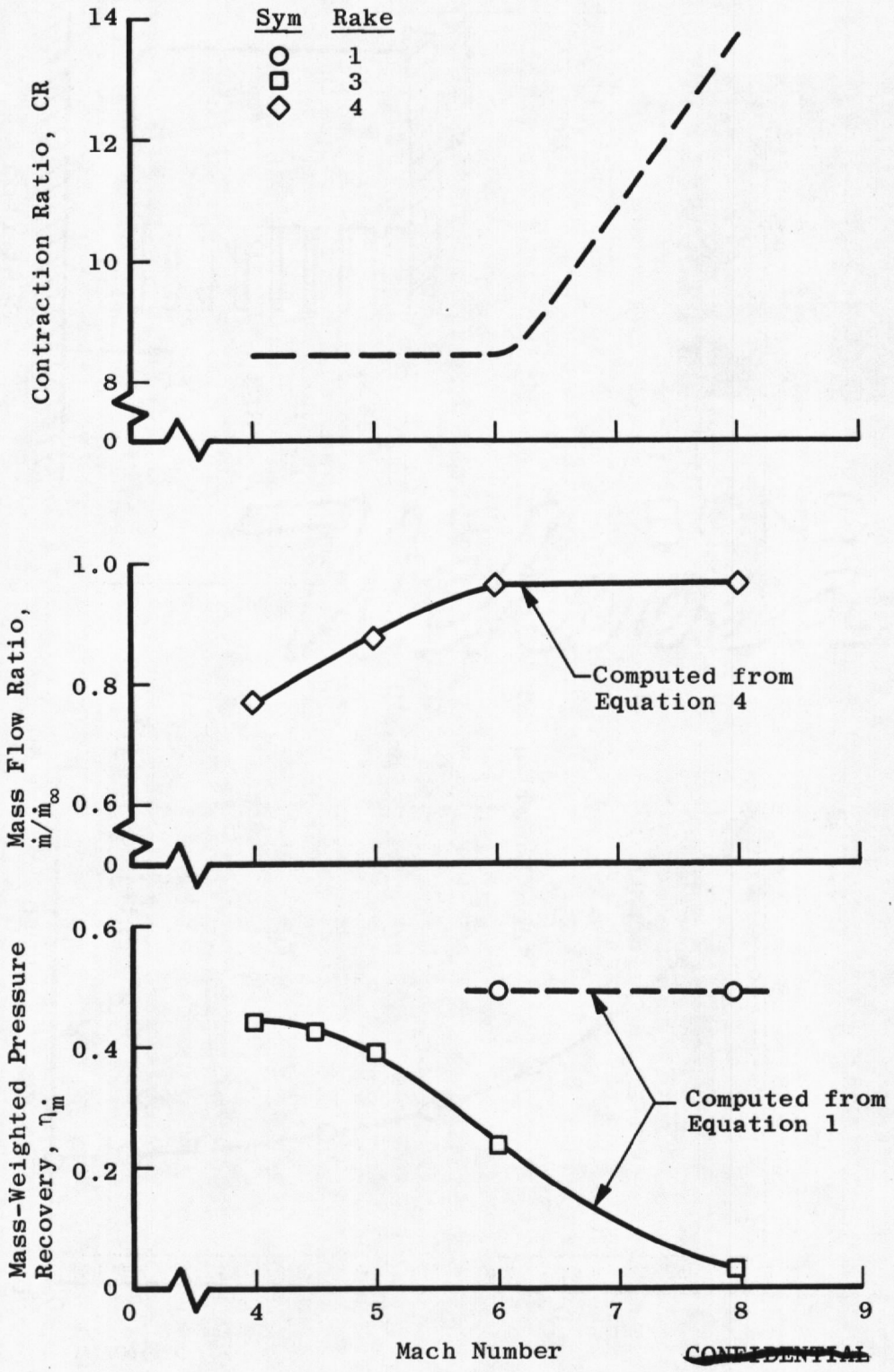

Fig. 17 Overall HRE Inlet Performance

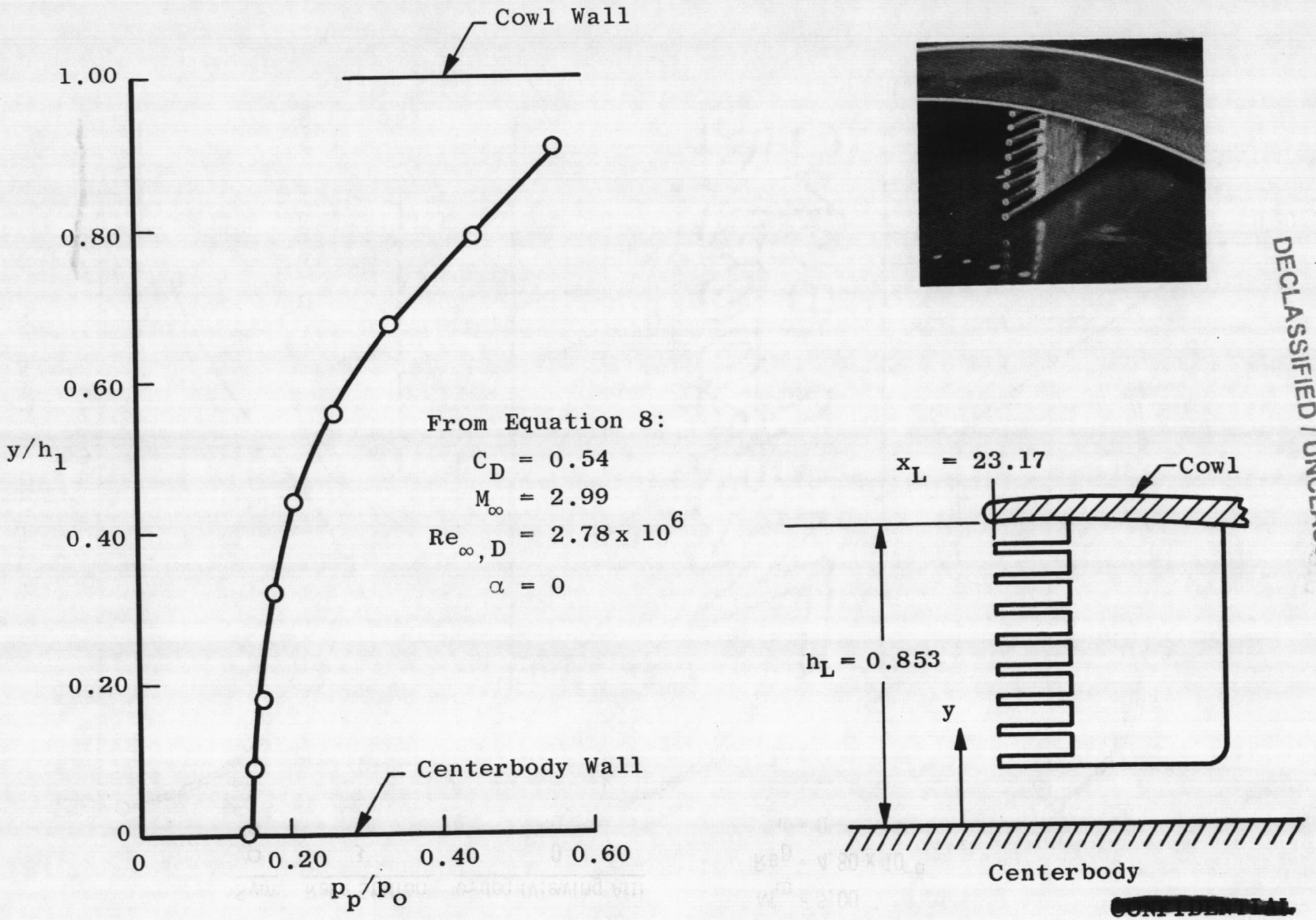

Fig. 18 Spillage Drag Rake Pitot Pressure Distribution

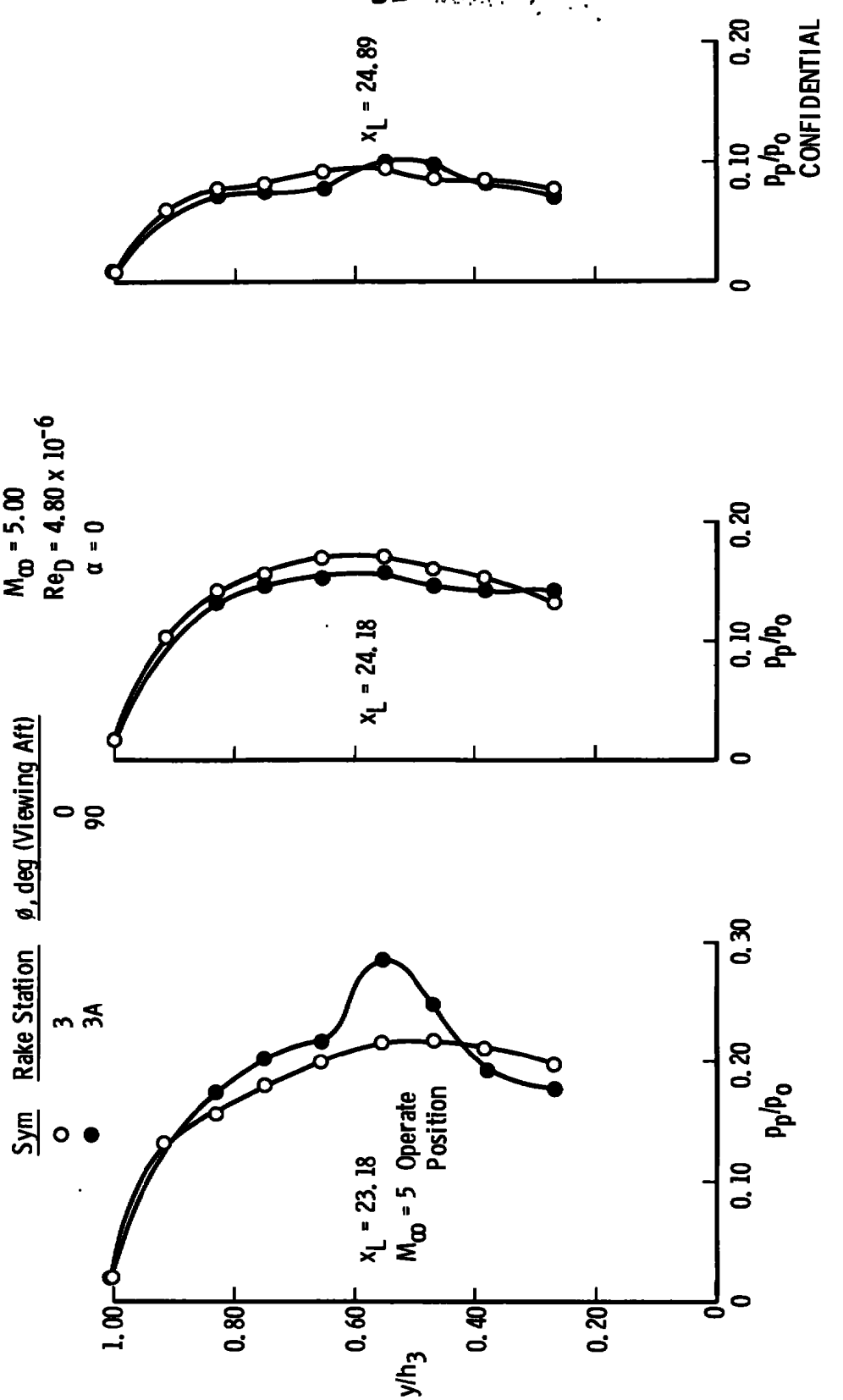

Fig. 19 Comparison of Rake 3 and 3A Pitot Pressure Distributions

The reverse side of this page is blank.

APPENDIX
TABLES

TABLE I
‡CONFIGURATIONS TESTED

Centerbody No.	Cowl Lip No.	Trip No.	Centerbody Doubler No.	Cowl Doubler
1	2	—	—	No
1	2	4	—	No
1	3	—	—	No
1	3	2	—	No
1	3	5	—	No
1	4	—	—	Yes
1	5	—	—	No
1	6	—	1,2,3	Yes
*1	7	—	—	Yes
1	7	—	1,2,3	Yes
1	7	—	3	Yes
1	7	6	—	Yes
1	7	7	—	Yes
1	7	8	—	Yes
1	7	9	—	Yes
2	1	2	—	No
2	2	1	—	No
2	3	—	—	No
2	3	2	—	No
2	3	3	—	No

‡All these configurations were tested for their starting characteristics at Mach number 4.

*Final configuration tested at M_∞ = 4 to 8.

UNCLASSIFIED

TABLE II
TEST SUMMARY

M_∞	p_o, psia	T_o, °R	$Re_{\infty,D} \times 10^{-6}$	p_∞, psia	α, deg	x_L, in.	K, in.
2.99	23	660	2.76	0.636	0, ±3	23.17	3.74
4.01	30	660	2.08	0.195	0	23.18	0.85
					0		1.13
					±3		1.24
					0, ±3		1.74
					0, ±3, ±5		3.72
					0, ±3, ±5	23.96	3.72
					0, ±3, ±5	24.90	3.72
					0, ±3, ±5	25.90	3.72
4.02	50	720	3.44	0.321	0	23.28	3.72
4.03	73	720	4.80	0.462	0	23.18	1.62
					±3		1.76
					0, ±3		3.72
					0	23.96	3.72
					0	24.98	3.72
4.53	110	660	5.76	0.366	0	23.24	3.74
5.00	40	660	1.66	0.076	0	23.18	0.81
					0, ±3, ±5		1.29
					0, ±3, ±5		1.50
					0, ±3, ±5		3.72
					0, ±3, ±5	24.20	3.72
					0, ±3, ±5	24.88	3.72
					0	25.87	3.74
	115		4.80	0.217	0, ±3, ±5	23.18	1.13
					0		1.44
					0		1.67
					0, ±3, ±5		3.73
					0, ±3, ±5	24.20	3.73
					0, ±3, ±5	24.89	3.73
6.01	75	850	1.44	0.047	0	23.14	0.68
					0		0.98
					0		2.17
					0		3.74
					0, ±3	23.24	0.68
					±4		0.77
					-4		0.82
	75	850	1.44	0.047	±3	23.24	0.96
					0, 4		1.02
					0, ±3		2.24
					0, ±3, ±4, 5		3.75

UNCLASSIFIED

TABLE II (Continued)

M_∞	p_o, psia	T_o, °R	$Re_{\infty,D} \times 10^{-6}$	p_∞, psia	α, deg	x_L, in.	K, in.
6.01	75	850	1.44	0.047	0	23.87	0.78
					0		0.92
					0		1.64
					0		3.74
					0	24.47	0.53
					0		0.67
					0		1.36
					0		3.74
					0	25.46	3.75
6.05	225		4.03	0.135	0	23.14	0.86
					0		0.99
					0		2.26
					0		3.74
					0	23.28	0.87
					0, -3		0.96
					±3		1.11
					±3		2.17
					0		2.32
					0, ±3, -4		3.72
					0, ±4.5	23.31	1.00
					0, -3, ±4.5		1.10
					0, -3, ±4.5		3.74
					0	23.87	0.87
					0, ±3		0.97
					0		2.16
					0		3.74
					0	24.49	1.10
7.93	225	1250	1.08	0.024	0	24.42	0.99
					0		1.30
					0	24.54	0.92
					0, ±3, ±5		1.27
					0, ±3, ±5		3.74
					0	24.66	0.92
	250		1.20	0.027	0		1.25
					0	24.52	3.74
					0	24.58	1.12
					5		3.71
8.00	650	1320	2.88	0.066	0	24.44	1.80
					0	24.57	1.44
					0		1.59
					-3		1.74
					-5		2.25
					3		2.55
					-3		3.74
					0	24.69	1.63

UNCLASSIFIED

TABLE II (Concluded)

M_∞	p_o, psia	T_o, °F	$Re_{\infty,D} \times 10^{-6}$	p_∞, psia	α, deg	x_L, in.	K, in.	Gas (Fuel)
5.99	60	850	1.08	0.038	0	23.32	3.72	N_2
↓	↓	↓	↓	↓	↓	↓	↓	He
6.03	175	↓	3.12	0.107	0	↓	↓	N_2
↓	↓	↓	↓	↓	0, ±3, ±5	↓	↓	He
7.93	225	1250	1.08	0.024	0	24.43	↓	N_2
↓	↓	↓	↓	↓	0, ±3	24.54	↓	N_2
↓	↓	↓	↓	↓	0	24.54	0.56	N_2
↓	↓	↓	↓	↓	0	24.58	3.72	He
↓	↓	↓	↓	↓	0	24.67	↓	N_2

UNCLASSIFIED

UNCLASSIFIED
Security Classification

DECLASSIFIED / UNCLASSIFIED

DOCUMENT CONTROL DATA - R & D

(Security classification of title, body of abstract and indexing annotation must be entered when the overall report is classified)

1. ORIGINATING ACTIVITY *(Corporate author)* Arnold Engineering Development Center ARO, Inc., Operating Contractor Arnold Air Force Station, Tennessee	2a. REPORT SECURITY CLASSIFICATION [redacted] 2b. GROUP 4

3. REPORT TITLE
WIND TUNNEL TESTS OF A TWO-THIRDS SCALE NASA HRE INLET AT MACH NUMBERS 4, 5, 6, AND 8 (U)

4. DESCRIPTIVE NOTES *(Type of report and inclusive dates)*
March 28 to September 18, 1968 - Final Report

5. AUTHOR(S) *(First name, middle initial, last name)*
Frederick K. Hube and Paul J Bontrager, ARO, Inc.

6. REPORT DATE	7a. TOTAL NO. OF PAGES	7b. NO. OF REFS
February 1969	59	3

8a. CONTRACT OR GRANT NO. F40600-69-C-0001	9a. ORIGINATOR'S REPORT NUMBER(S) AEDC-TR-69-9
b. PROJECT NO. 9325	
c. Program Area 921E	9b. OTHER REPORT NO(S) *(Any other numbers that may be assigned this report)*
d.	N/A

10. DISTRIBUTION STATEMENT In addition to security requirements which must be met, this document is subject to special export controls and each transmittal to foreign governments or foreign nationals may be made only with prior approval of NASA Langley Research Center, Langley AFB, Virginia 23365

11. SUPPLEMENTARY NOTES	12. SPONSORING MILITARY ACTIVITY
Available in DDC	NASA Langley Research Center Langley AFB Virginia 23365

13. ABSTRACT

An axisymmetric, variable geometry, two-thirds scale model of a NASA Hypersonic Research Engine (HRE) inlet was tested at Mach numbers 4, 5, 6, and 8. Surface pressures and temperatures were measured on the inlet centerbody and inside the cowl. Pitot pressure measurements were made at four stations along the internal passage. The measurements were obtained for various cowl positions at free-stream Reynolds numbers from 1.08×10^6 to 5.76×10^6 (based on a 12-in. cowl diameter) and over an angle-of-attack range from -5 to +5 deg. The model walls were internally cooled and maintained at a minimum frost-free condition at each test condition. Selected results are presented to illustrate the effects of cowl position, angle of attack, Mach number, and Reynolds number on the surface and rake station measurements. Inlet performance data at design operating conditions are also presented. (U)

This document is subject to special export controls and each transmittal to foreign governments or foreign nationals may be made only with prior approval of NASA Langley Research Center, Langley AFB, Virginia 23365.

This document has been approved for public release its distribution is unlimited.

DD FORM 1 NOV 65 1473

UNCLASSIFIED
Security Classification

DECLASSIFIED / UNCLASSIFIED

14. KEY WORDS	LINK A ROLE	LINK A WT	LINK B ROLE	LINK B WT	LINK C ROLE	LINK C WT
intake systems						
NASA Research Engine						
wind tunnel tests						
hypersonic flow						
pressure distribution						
temperature distribution						

1. Air inlets -- HRE
2. " " -- Performance
3. " " -- Pressure distribution
4. " " -- Temperature "

1-2